INVESTIGATION INTO THE CONTRIBUTION OF NEUTRAL HYDROGEN MASS IN GALAXY CLUSTER BY USING SMALL RADIO TELESCOPE

MOHD SHAIFUL RIZAL BIN HASSAN

FACULTY OF SCIENCE
UNIVERSITY OF MALAYA
KUALA LUMPUR

2017

INVESTIGATION INTO THE CONTRIBUTION OF NEUTRAL HYDROGEN MASS IN GALAXY CLUSTER BY USING SMALL RADIO TELESCOPE

MOHD SHAIFUL RIZAL BIN HASSAN

DISSERTATION SUBMITTED IN FULFILMENT OF THE REQUIREMENTS FOR THE DEGREE OF MASTER IN SCIENCE

FACULTY OF SCIENCE
UNIVERSITY OF MALAYA
KUALA LUMPUR

2017

UNIVERSITY OF MALAYA

ORIGINAL LITERARY WORK DECLARATION

Name of Candidate: Mohd Shaiful Rizal Hassan

Registration/Matric No: SGR110020

Name of Degree: Degree of Master in Science

Title of Project Paper/Research Report/Dissertation/Thesis ("this Work"):

Investigation into the Contribution of Neutral Hydrogen Mass in Galaxy Cluster by Using Small Radio Telescope

Field of Study:

Astronomy & Astrophysics

I do solemnly and sincerely declare that:

(1) I am the sole author/writer of this Work;
(2) This Work is original;
(3) Any use of any work in which copyright exists was done by way of fair dealing and for permitted purposes and any excerpt or extract from, or reference to or reproduction of any copyright work has been disclosed expressly and sufficiently and the title of the Work and its authorship have been acknowledged in this Work;
(4) I do not have any actual knowledge nor do I ought reasonably to know that the making of this work constitutes an infringement of any copyright work;
(5) I hereby assign all and every rights in the copyright to this Work to the University of Malaya ("UM"), who henceforth shall be owner of the copyright in this Work and that any reproduction or use in any form or by any means whatsoever is prohibited without the written consent of UM having been first had and obtained;
(6) I am fully aware that if in the course of making this Work I have infringed any copyright whether intentionally or otherwise, I may be subject to legal action or any other action as may be determined by UM.

Candidate's Signature Date:

Subscribed and solemnly declared before,

Witness's Signature Date:

Name:

Designation:

ABSTRACT

A single pointing observation by using small radio telescope is considerably important in tracing the amount of neutral hydrogen (HI) in cluster of galaxies as a whole. This spectral line analysis, centered at 21-cm provides an insight of the HI behaviour in clusters of galaxies. Cluster A262 has been chosen as the best candidate for the study because of its properties that fit with the instrument's capability and source's visibility at the location of the telescope. In addition, the chosen of A262 is based on the characteristics such as (a) it is a spiral rich cluster and (b) it is distributed unevenly throughout the edge of the cluster, which represents a good approximation of HI mass (M_{HI}) location. Several spectra have been identified that show significant detection from A262, which peaked near to source velocity, 4890 km/s. The study has shown that 21-cm spectral line observation by using small radio telescope yields the source velocity, v = 4970 km/s (slightly different from literature) which contribute to HI mass of about $M_{HI} = (6.22 \pm 0.32) \times 10^{11}\ M_{\odot}$. The estimated M_{HI} is then being compared with virialized mass of the cluster, M_{VT}. M_{VT} indicates the total mass of the cluster which is obtained from spectroscopic analysis – $M_{VT} = (7.16 \pm 0.09) \times 10^{13}\ M_{\odot}$. Spectroscopic analysis also provides the information of how HI mass being distributed in the cluster – by determining the location of HI rich galaxies resides in the cluster. Finally, the contribution of dark matter mass, M_{DM} in A262 has been deduced, which is believe to be the major building block for most of clusters of galaxies (~ 97%). All the results presented in this study were compatible with previous studies and meet the objectives of the study. Thus, the technique used in this study is then quantified as reliable, rather than using a raster scanning, which is more suitable for observation on individual galaxy.

ABSTRAK

Satu pemerhatian menunjuk tunggal dengan menggunakan teleskop radio kecil adalah penting dalam mengesan jumlah hidrogen neutral (HI) dalam kelompok galaksi secara keseluruhannya. Analisis garis spektrum, berpusat pada 21-sm menyediakan pengesanan kelakuan HI dalam kluster galaksi. Kluster A262 telah dipilih sebagai calon terbaik untuk kajian ini kerana sifat-sifat yang sesuai dengan keupayaan instrumen dan kebolehtampakan objek di lokasi teleskop. Di samping itu, yang dipilih daripada kluster A262 adalah berdasarkan kepada ciri-ciri seperti berikut (a) ia merupakan satu kluster yang kaya dengan galaksi lingkaran dan (b) galaksi-galaksi tersebut bertaburan sama rata di seluruh pinggir kluster, yang mewakili penghampiran yang baik kepada penentuan jisim HI. Beberapa spektrum telah dikenal pasti yang menunjukkan pengesanan penting dari kluster A262, yang memuncak berhampiran dengan halaju kluster galaksi iaitu, 4890 km/s. Kajian ini telah menunjukkan bahawa pemerhatian garis spektrum pada 21-sm dengan menggunakan teleskop radio kecil menghasilkan halaju kelompok galaksi, v = 4970 km/s (sedikit berbeza daripada kajian literatur) yang menyumbang kepada jisim HI iaitu lebih kurang $(6.22 \pm 0.32) \times 10^{11}\ M_{\odot}$. Anggaran jisim HI kemudiannya dibandingkan dengan jisim virial kluster, M_{VT}. M_{VT} menunjukkan jumlah jisim kelompok yang diperolehi daripada analisis spektroskopi – $M_{\mathrm{VT}} = (7.16 \pm 0.09) \times 10^{13}\ M_{\odot}$. Analisis spektroskopi juga menyediakan maklumat bagaimana jisim HI bertaburan dalam kluster - dengan menentukan lokasi galaksi kaya dengan HI berada di dalam kluster. Akhir sekali, sumbangan jisim jirim gelap dalam A262 telah dihitung, yang dipercayai adalah blok binaan utama bagi kebanyakan kluster galaksi (~ 97%). Semua keputusan yang dibentangkan dalam kajian ini adalah bersesuaian dengan kajian sebelum ini dan memenuhi objektif kajian. Oleh itu, teknik yang digunakan dalam kajian ini kemudiannya dikira sebagai sah, berbanding dengan menggunakan imbasan raster, yang lebih sesuai untuk pemerhatian di galaksi individu.

ACKNOWLEDGEMENTS

First and foremost, I gratefully acknowledge the support and guidance of my supervisor, Associate Professor Dr. Zamri Zainal Abidin, without which the study could have not been completed. I am deeply indebted by the help and assistance given by: Dr. Christine Jordan from Jodrell Bank Observatory (United Kingdom), for the permission to use the telescope for the study; Associate Professor Melanie Johnston-Hollitt from Victoria University of Wellington (New Zealand), for the spectroscopic analysis on the archival data; and Professor Peter Thomasson from University of Manchester (United Kingdom), for the advice in the instrumentation part. I thank the members of Radio Cosmology Research Laboratory, for their cooperation and contribution throughout the study, especially the members of Dark Matter Group. Without exceptional, my thousand thanks to my family members – especially my mother – and friends who paved the path before me upon whose shoulders I stand.

TABLE OF CONTENTS

LIST OF FIGURES

LIST OF TABLES

LIST OF SYMBOLS AND ABBREVIATIONS

For example:

k	:	Boltzmann constant: 1.381×10^{-23} m^2 kg s^{-2} K^{-1}
M_{DM}	:	Dark Matter Mass
ISM	:	Interstellar Medium
ICM	:	Intracluster Medium
G	:	Gravitational Constant: 6.674×10^{-11} m^3 kg^{-1} s^{-2}
HI	:	Neutral Hydrogen
M_{HI}	:	Neutral Hydrogen Mass
$L_{\odot}$	:	Solar Luminosity: 3.828×10^{26} W
$M_{\odot}$	:	Solar Mass: 1.989×10^{30} kg
ΣM_i	:	Total Stellar Mass
σ	:	Velocity Dispersion
M_{VT}	:	Virialized Mass
R_{V}	:	Virialized Radius

LIST OF APPENDICES

CHAPTER 1 INTRODUCTION

1.1 Research Background

The Universe can be interpreted as a supergiant structure containing multi-billion galaxies started to scatter around 13.8 billion years ago, and consists of galaxies, planets, stars, interstellar medium (ISM) as well as intracluster medium (ICM). It shows no boundary or in other words the size of the Universe is infinitely finite (Hartle & Hawking, 1983). Since the time of Big Bang, which is believed to be an initial point of the formation of the Universe, the space-time is continuously expanding (Slipher, 1917 & Hubble, 1923), based on the spectroscopic observation of the galaxies being far away from each other – or redshifted – at increasing rate or the Universe is accelerating (Perlmutter, Schmidt & Riess, 2011). However, some of the galaxies in the Universe show blueshifted – where it is approaching our home galaxy, Milky Way. For example, the Andromeda Galaxy or M31 is approaching towards us (Slipher, 1913; Cox & Loeb, 2008) at velocity approximately 120 km/s (Binney & Tremaine, 2007) and could cause great collision which is expected to take place in about 4 billion years from now. Large ratio of receding:approaching for nearby galaxies (Slipher, 1917) remarkably shows that space-time universe is expanding.

As the Universe is expanding and occurs in every point in the Universe, consequently, the Universe appears to be the same throughout the field and appears to be the same in every direction or viewing angle when we stand at any point in the Universe. These characteristics, scientifically know as homogeneous and isotropic, respectively, are based on the work by Friedmann-Lemaitre-Robertson-Walker (FLWR metric), developed between 1920's – 1930's essentially extracted from Einsten's field equation of general relativity (Einstein, 1915) and sometimes called the Standard Model (SM) of modern cosmology. The Lambda-CDM (or Λ-CDM) model is the simplest

model of SM because the model caters a sensibly perfect match for the observation of the accelerating expansion of the Universe observed in the light from distant galaxies and supernovae (Caldwell et al., 1998; Frieman, Turner & Huterer, 2008; Kroupa et al., 2010; Planck Collaboration et al., 2016).

The large scale of Universe could be portrayed as a sequence of superclusters extended beyond 100 Mpc – as for the largest supercluster – separated by huge voids. By zooming in the scale of the superclusters to clusters of galaxies, we will see them as a field containing bunches of galaxies distributed diffusely. Clusters of galaxies have been studied extensively for their intrinsic properties, the baryonic content of the Universe, large-scale structure, evolution and cosmology (Zwicky, 1958; Bahcall, 1977, 1988, 1996; Oort, 1983; Dressler, 1984; Rood, 1988 and Peebles, 1993). Furthermore, cluster of galaxies is a potential trigger point for the heated debate among scholars in cosmology, especially related to dark matter searches. Dark matter or initially known as invisible matter (due to its invisibility from our sight and non-detectable in any windows of electromagnetic spectrum) was believed to exist because of some reasons that affect the dynamical structure of clusters of galaxies (Chapter 2). Initial previous studies showed that the total mass of individual galaxies in clusters of galaxies alone was insufficient to account the mass of the gravitational potential energy that prevent all the galaxies from flying apart – in which the total mass of the clusters of galaxies can be determined by using virial theorem (Zwicky, 1933, 1937).

As Zwicky did for Coma cluster by using virial analysis, it shows that the similar trend also occurred in Virgo cluster (Smith, 1936). Both Zwicky and Smith calculated the velocity dispersion of each galaxy in the clusters and found that the motions of the galaxies are much faster to keep them bounding in a great gravitational potential well. However, the gravitational effects from neighbouring galaxies were inadequate to

explain the peculiar motions of the galaxies in the cluster. The lack of total mass that contributes from individual galaxies alone also was deficient to explain the bending of light from background object that travel through massive clusters of galaxies (Einstein, 1936) – where Zwicky also proposed this idea in his remarkable 1937 paper. In order to account for an extra mass in clusters of galaxies, scientist came out with the idea of hypothetical particles that also contribute to the total mass of the clusters of galaxies and therefore to reconcile the strange dynamical structure in clusters of galaxies. Rather than its presence observed in clusters of galaxies, dark matter also were believed to exist in the Solar neighborhood (Oort, 1932, 1960), spiral galaxies (Rubin et al., 1970) and the entire Universe (Penzias & Wilson, 1964).

Another significant method in justifying the existence of dark matter is to look at mass-to-luminosity (M/L) ratio which represents the total mass should be accounted for a given luminosity, first initiated by Schechter, 1976. In Hertzsprung-Russell's diagram, the luminosity of the stars was plotted against the size which corresponding to their masses. It shows that the M/L ratio for different type of stars varied in such a way that massive stars have small value of M/L, while smaller stars have large value of M/L. This variation indicates that if we would like to find out the total mass of a galaxy containing a number of stars, it can be deduced from the total luminosity of each star in the galaxy yielding total luminosity. It turns out that for an "ideal" galaxy it has M/L equal to M/L of the Sun ($M_\odot/L_\odot$) corresponding to factor of 1 appeared in front or $M/L = M_\odot/L_\odot$ and shows the absence of dark matter. However, for our home galaxy Milky Way, the M/L is about 50 – 90 $M_\odot/L_\odot$ (Faber & Gallagher, 1979; Bell & de Jong, 2001) – a factor appeared symbolizes that there is an extra mass contained in the galaxy for a given luminosity. This is also true for clusters of galaxies where typical clusters of galaxies have M/L of about 250 – 300 $M_\odot/L_\odot$ (Girardi et al., 2000), obviously means that there is a huge amount of dark matter present in clusters of galaxies. Based on current

calculations, dark matter constitutes almost 27% of the total content of the Universe (e.g. Carroll, 2007; Matthew, 2013; Planck Collaboration et al., 2013) and more than 70% of this matter resides in clusters of galaxies.

The entire Universe is build up from both visible and invisible matter, so for the clusters of galaxies. Since dark matter is said to be the major building block for invisible matter, meanwhile major visible matter is coming from the contribution of neutral hydrogen (HI). Although the HI atoms are actually rare, the clouds of HI are largely confined to gravitational potential wells with relatively high density environment, which makes the clouds lose their capability to running through photoionization process (Briggs, 2003). Thus, the HI clouds will collapse to turn into star formation region and associates closely to galaxies. The HI clouds are also observed exist in the form of intergalactic atomic hydrogen in clusters of galaxies and provides the determination of total HI mass and its distribution in clusters of galaxies (Koehler & Robinson, 1966; Dahlem, 2005; Ibrahim, Abidin & Hassan, 2017 (*in prep.*)). The HI emission and absorption lines can be observed in specific spectral line of electromagnetic spectrum. In addition, the 21-cm hyperfine line in clusters of galaxies as a whole indicate that the missing mass or dark matter mass is not in the form of HI (Haynes et al., 1978). It has been proven that the percentage of HI gas together with hot gas – which visible in X-ray band – in clusters of galaxies is estimated to be about 15 – 20%, while the contribution of stars and galaxies only about 3 – 5%.

The resulting of HI radiation is due to the interaction between proton and electron when the electrons overcome the altering of spinning orientation with respect to proton spin (Chapter 2). The 21-cm which corresponds to frequency emitted at 1.42 GHz is considered as thermal radiation since it is arising from a population distribution of energy levels that is in local thermodynamics equilibrium with the gas in the cloud

(Pratap & McIntosh, 2005). Moreover, the 21-cm spectral line observation also provides extra information of precisely determination of redshifts, *z*, from the midpoint velocity and the HI line width is the rotational velocity indicator that most commonly used in the Tully-Fisher (TF relation) as a secondary distance application (Haynes et al., 1997). The HI spectral line observation on clusters of galaxies can be done using single radio telescope or an array (combination of a few radio telescopes sorted in a certain configuration) equipped with a 21-cm receiver and produced wider beam-width pattern. This study was carried out in conjunction of looking at the contribution of HI mass into the total mass of cluster of galaxies.

1.2 Problem Statement

This research was carried out due to some problems involving the evolution of the Universe. As mentioned earlier in Section 1.1, the important parameter M/L for a typical cluster is about 250 – 300 $M_{\odot}/L_{\odot}$. This value also indicates that actually the mass of the clusters somehow exceeds the visible mass from the contribution of galaxies (< 10%) and intracluster gas (10 – 25%) that can be observed in electromagnetic bands. If we compute the total individual mass of the galaxies in the cluster alone, it is insufficient to describe the peculiar motion of the galaxies in the cluster. From the analysis of virial theorem, we can estimate the total gravitational mass, M_{VT} (or total mass) that keeps all the galaxies bound together without flying apart. The application of virial theorem makes use of velocity dispersion (σ) analysis since it is related to the equation below:

$$M_{\mathrm{VT}} = \frac{3\pi\sigma^2 R_{\mathrm{V}}}{2G} \tag{1}$$

where R_{V} is the virial radius (typically 2 Mpc), G is the gravitational constant and σ is the velocity dispersion which differs based on the richness class that the cluster belongs to and can be defined as $\sigma = [< (v_i - <v>)^2 >]^{-1/2}$, where v_i is the velocity of individual

galaxy. M_{VT} for different type of cluster is varied as follows: rich cluster, $10^{15} – 10^{14}$ $M_{\odot}$; intermediate cluster, $10^{14} – 10^{13}$ $M_{\odot}$; and poor cluster, less than 10^{13} $M_{\odot}$ (Voit, 2005). This value is compatible with the mass that we can trace by using X-ray observation since it actually gives rise to the actual total mass in the cluster. Hence, we can say that M_{VT} is equivalent to the total mass of the cluster in a given radius. Definitely, the techniques and instruments used for X-ray observation are different from the application of virial theorem. For the example of Coma cluster, M_{VT} has been calculated to be about 10^{15} $M_{\odot}$ (since the cluster falls into rich cluster type) and implies high M/L ratio of 250 $M_{\odot}/L_{\odot}$.

The neutral hydrogen mass, M_{HI}, describes the total neutral hydrogen content or baryonic component in the cluster. The distribution of M_{HI} depends on the distribution of different morphological type of galaxies in the cluster. It is well-known that the most HI rich galaxies are found in spirals (S) rather than in ellipticals (E) and lenticulars (S0). The classification of cluster's type based on Bautz-Morgan, whether it is regular or irregular cluster; state that the distribution of different morphological type affects the allocation of HI in clusters. Thus, the distribution of HI depends on the way of spirals scattered around in the clusters. In other words, more HI can be found in the cluster with higher percentage of spirals for the same type of BM classification and more concentrated at the edge of the cluster if the spirals located at the outskirts of the cluster rather than at the centre.

In this study, the values of M_{VT} and M_{HI} have been estimated and so for the rough estimation of the dark matter mass or M_{DM}, which is said to be responsible for the odd dynamical behavior in the cluster. Based on the earlier assumption, we have already known that M_{VT} should be higher than that of M_{HI} ($M_{VT} > M_{HI}$). If $M_{VT} = M_{HI}$, thus we conclude that the cluster contains no extra mass and the theory of dark matter could be

wrong. However, by considering previous studies analysis, this is not the case since the role of dark matter that contributes to the total mass of the cluster should not be omitted. Hence, the work is based on the statement that $M_{VT} > M_{HI}$, since cluster does not contain only HI but also any other components based on the equation below:

$$M_T \equiv M_{VT} = M_{DM} + M_{HI} + \Sigma M_i \quad (2)$$

or

$$M_{DM} = M_{VT} - (M_{HI} + \Sigma M_i) \quad (3)$$

where M_T is the total mass of the cluster which equivalent to M_{VT} and ΣM_i is the total individual galaxies – or total stellar mass – contain within the cluster boundary. The percentage of M_{HI} also can be estimated to see how much M_{HI} contribute to the accumulated mass of the cluster.

1.3 Research Objectives

The objectives of the study have been highlighted as follows:

(a) To estimate the M_{HI} of galaxy cluster A262

The value of M_{HI} can be found by invoking nearly similar concept in Battye et al., 2004. They had tabulated the configuration of radio telescopes based on the collecting area and the synthesized beam produced by those configurations. From the analysis of the configurations, they implied that bigger collecting area of the array will yield smaller full-width-half-maximum synthesized beam pattern, θ_{FWHM} and instantaneous field-of-view (FOV), Ω_{inst}. Although the work applied an array or interferometer technique rather than single dish that has been used in this study, the total collecting area of the configuration (or parabolic dish) will affect the value of θ_{FWHM} and Ω_{inst} in which they show similar trends (Chapter 3). This technique has been implemented to

find M_{HI} for the whole cluster (depends on the limitation of the instrument to cover cluster's area) and applied standard formula (e. g. Roberts, 1975) that relates M_{HI} and the observed flux density, S_v, obtained from 1.42 GHz spectral line observation, integrated over a velocity width, dv, given as:

$$\frac{M_{HI}}{M_{\odot}} = (2.35 \times 10^5)\frac{1}{1+z}\ d_L^{\,2} \int S_v \, dv \qquad (4)$$

where d_L is the luminosity distance to redshift z.

The chosen of this concept is to test its validity for a single radio telescope observation. The concept has not yet been tested for single observation and using small radio telescope. If the concept works well for this study, we can conclude that the concept is valid for both single and interferometer observation.

(b) To analyze M_{VT} by using virial theorem based on the velocity dispersion analysis

The application of virial theorem is vital for clusters since it will give the estimation value of M_T. However, the determination of M_{VT} will depend on the capability of the instrument to cover FOV of the cluster. This is because only a specific number of galaxies that bounded within the area of the beam pattern produced by the telescope should be taken into account. Spectroscopic analysis also has to be applied in order to determine cluster membership and a review on velocity dispersion of each member should be done in applying virial theorem. Then, the values of M_{VT} and M_{HI} should be compared and M_{DM} can be directly obtained by using equation (3).

(c) To identify the distribution of HI mass in galaxy cluster A262

The location of M_{HI} has to be determined because it leads to the information of HI concentration at different sites in the cluster. Since M_{HI} depends on the distribution of spirals in the cluster, the inspection on the diversity of different morphological types of galaxies in the cluster is crucial.

(d) To determine the upper limit of dark matter mass in galaxy cluster A262

The usage of single-pointing observation by using small radio telescope is hoped to provide an upper limit of dark matter mass estimation. Since dark matter mass is the main component of most of galaxy clusters, high percentage of dark matter mass is expected from this study i.e. more than 80%.

1.4 Research Hypothesis

In this study, a few hypotheses have been tested. The hypotheses are:

(a) Dark matter contribution in galaxy cluster can be deduced by relying on M_{HI} estimation using small size radio telescope equipped with 21-cm receiver,

(b) $M_{VT} > M_{HI}$ since $M_T \equiv M_{VT} = M_{DM} + M_{HI} + \Sigma M_i$ and

(c) most of the M_{HI} resides at the periphery of the cluster.

1.5 Significance of Study

The study is wished to use a new and novel method of using small radio telescope to trace the contribution of M_{HI} in cluster of galaxies, particularly A262. The study implied the method that has not been done before, i.e. to look at the cluster as a whole in HI band. This technique, if successful, would lead to a significant extensive study on several other clusters of galaxies nearby. Additionally, this technique can be used in determining the upper limit of dark matter contribution in large scale of cluster of galaxies.

CHAPTER 2 LITERATURE REVIEW

2.1 The Radio Window

Unconcealed the timeline of radio astronomy brings us back to the early of the twentieth century when the detection from extraterrestrial object was first discovered at Bell Telephone Laboratories, USA by Karl Guthe Jansky (1905 – 1950) where his name is honored by radio astronomers for the strength of radio sources (or radio flux density). Before his success, several attempts were done by Sir Oliver Lodge (1851 – 1940) and Charles Nordmann (1881 – 1940) in proving the evidence of radio emission from the Sun and other astronomical objects. However, that attempt met failure because during that time the electronic art and knowledge had not advanced sufficiently to meet victory. Though they failed to justify their inference, some of the important knowledge in radio astronomy has been used widely around the globe in enhancing the quality of the observation such as the chosen of the best observing site with interference-free by Lodge.

Jansky triggered the development of modern radio astronomical observation in which several people was extending his work broader. One of the people who investigated Jansky's work was Grote Reber (1911 – 2002), the first person who conducted first sky survey in the radio frequencies band. In his backyard, he built his own parabolic dish in 1937 with diameter of 9 meters. By using his radio telescope, he tried several times to detect signals from outer space at several windows in radio frequencies. Nevertheless, in 1938, he only made a success at his third attempt when he discovered radio signal at 160 MHz, confirming Jansky's discovery. Another person who continued Jansky's work was John D. Kraus (1910 – 2004). Kraus has invented various types of antenna for radio astronomical purposes. He commenced radio observatory at Ohio State

University, used to carry out the Ohio Sky Survey and also active in writing a textbook in radio astronomy.

Our understanding about the behaviour of electromagnetic spectrum has been extended from the beginning of 20th century until recent time, and it becomes more importance in investigating the behaviour of the Universe by studying spectroscopic characteristics of emission and absorption lines of electromagnetic waves. It is well known that electromagnetic spectrum is a mixture of various types of wavelength, allowed us to study the emission of any terrestrial objects in different portion of wavelength such as optical, infrared, X-ray as well as radio. At present day, with the advancement and modification of astronomical instrumentations allows us to view the Universe in a wide range of frequencies, creating immense number of mysterious question need to be answered.

One portion of wavelength currently active in studying the large scale of the Universe makes use of radio window or more often we used the term of radio astronomy. Radio frequencies emitted by any object in the outer space can penetrate the Earth's atmosphere and can be detected in radio window ranging from lower frequency limit of approximately 3 MHz (wavelength, $\lambda \sim 0.1$ m) until approximately 300 GHz ($\lambda \sim 1.0 \times 10^{-5}$ m) (Figure 2.1). Because of its extremely high penetration power, radio window allows us to receive high percentage of the signals radiated by celestial body in radio band – even though there are few percent of the radiation have been absorbed by atmosphere. The limitation of our eyes to receive the entire wavelength fell in radio window makes it invisible to us. To increase the power received by radio signals, instruments to study the radiation in radio frequency have been built in suitable region to provide more interesting features of our space we live in. Indeed, in the wide range of radio window there are some emission or absorption lines that we can observe and study

the characteristic of element that enveloped our Universe. The use of radio astronomy is important in explaining (just name a few): non-thermal radiation from our Galaxy and many other astronomical sources; thermal spectral-line emission from cold interstellar gas atoms, ions, and molecules; coherent maser line emission from interstellar ions and molecules; coherent continuum emission from stars and pulsars; cosmic microwave background radiation from the hot big bang; evidence for dark matter, deduced from the HI rotation curves of galaxies and gravitational lensing (Pratap & McIntosh, 2005).

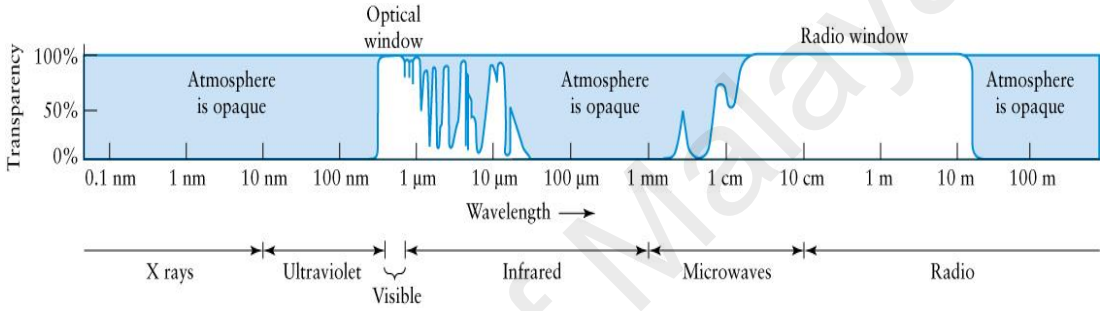

Figure 2.1 The variety of wavebands, ranging from X-ray up to radio and their transparency through Earth's atmosphere (Image credit: http://www.public.asu.edu/)

The study focused on a specific frequency of neutral hydrogen line, or HI line that lies at frequency of 1.42 GHz (λ = 21 cm). The selection of HI line study is based on the information that the most abundant element in the Universe is in the form of baryonic component, which composed of a proton and a neutron. It is also the simplest element in the Universe and also gives a boost for stars and galaxies formation. The resulting of HI radiation is due to the interaction between proton and electron when the electrons overcome the altering of spinning orientation with respect to proton spin (Figure 2.2), based on van de Hulst calculation in 1944. This process emits rest frequency at 1.42 GHz and is useful tool to measure the distribution of HI in the sky. As mentioned in Chapter 1, the 21-cm spectral line observation is considered as thermal radiation since it is arising from the interaction of the gas clouds with the population of different energy

levels in the local thermodynamic equilibrium. This emission also contributes to some of important finding in the study of the early Universe. According to big bang nucleosynthesis (BBNS) theory of Universe's early formation, stable protons and neutrons were created after the Universe cooled at a certain temperature and produced HI and this HI can be mapped by using suitable tools.

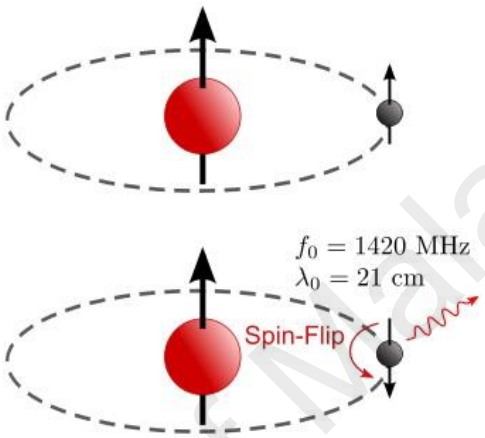

Figure 2.2 The altering spin of the electron results in the emission of photon that can be observed at rest frequency 1.42 GHz

In addition, HI spectral line observation is also useful for: quantification of overall mass and measurements of distances – either from Hubble's law (directly) or Tully-Fisher (TF) relation (indirectly). HI line emission profile also provides three important features: (1) the redshift is accurately determined from the midpoint velocity, (2) the integrated HI line flux gives an estimate of the total HI mass and (3) the HI line width is the rotational velocity indicator most commonly used in the TF secondary distance application (Haynes et al., 1997). In Jacqueline (2010), the 21 cm line of HI observation used to investigate the best evidence for ongoing gas accretion found in the lowest density environment, while removal of gas in highest density environments stops star formation and reddens the galaxies (Sarazin, 1988). Hence, it shows that the HI line observation is very useful tool for probing the evolution of galaxies in clusters of

galaxies as well. Schröder et al. (2001) used 21 cm line of HI to measure mass-to-light ratio of the galaxies. The 21-cm radiation measured is Doppler-shifted due to the relative velocity of the emitting matter along the line of sight. This pattern shows that clusters of galaxies observed at 1.42 GHz, contain missing component which is not in the form of HI gas (e. g. Haynes et al., 1978; Peterson, 1978; Baan et al., 1978 and Shostak et al., 1982). However, by relating the distribution of different morphological types in clusters of galaxies and its HI mass content, it can be used as a tracer to determine where the HI location in clusters of galaxies is (example in Figure 2.3). Because hydrogen is the most abundant element in galaxies and clusters of galaxies, and 21 cm radiation is insignificantly absorbed by dust or the atmosphere, the 21 cm line is a powerful tool for probing galaxies and clusters of galaxies.

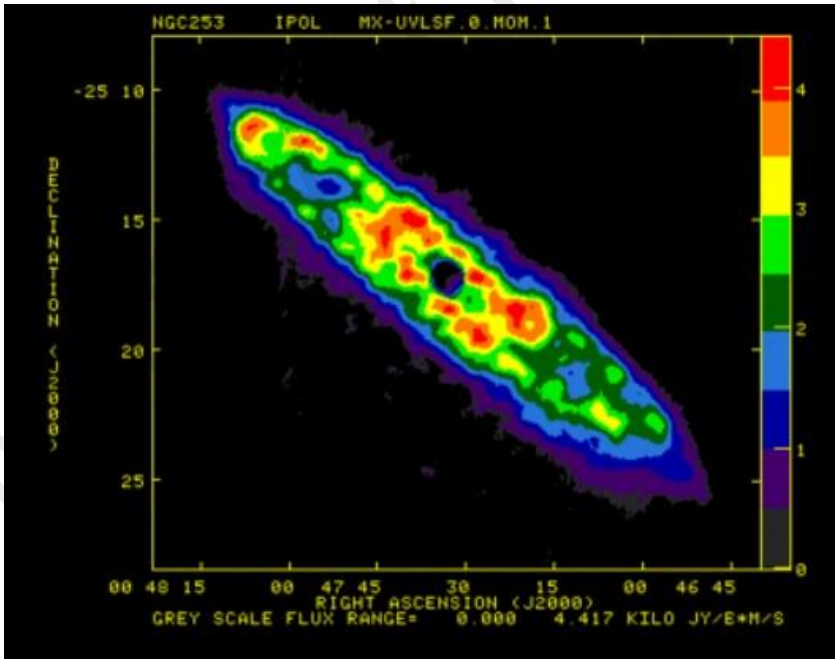

Figure 2.3 A 21-cm line image of the spiral galaxy NGC253 is shown in false colour. Regions with lots of HI are coloured red, while regions with very little HI detected are coloured purple (Image credit: Koribalski, Whiteoak & Houghton, 1995)

In conducting an astronomical observation in radio window, the researchers should locate up the instruments at a certain area based on several features to increases the eminence of the observation. In comparison with optical astronomical observation, most of the optical telescopes were established at high altitude; usually at the top of the mountain to reduce the amount of distortion of the image caused by the atmosphere and should be away from residential and commercial area to reduce light pollution. In radio astronomy, however, the main instrument used, i.e. radio telescopes should be located at the places which are free from radio frequency interference or RFI. RFI is defined as any internal or external 'unnecessary' signals received by the instruments that prevent high quality of 'necessary' signals to be produced, just like an atmosphere and light from a street lamp do in optical astronomy. The devices such as television, radio, computers and mobile phone generate RFI to radio astronomical observation. Thus, particular area for this research purposes should be considered as the main criteria to set up radio telescope. This particular area is called radio quiet zone or RQZ which is completely free from RFI.

Recent scientists around the globe, especially radio astronomers are looking forward to have instruments with higher sensitivity to study the characteristics and behavior of the Universe in more detail. In order to build up those instruments, they must also consider the best site for the instrument to be located under collaborations of few countries around the world. After several criteria have been implemented for the best location in the project, Australia and South Africa was chosen as an ideal place to build up multi-million dollar projects of Square Kilometers Array or SKA. Australia (New Zealand as a partner) was selected for low frequencies radio observation while South Africa for higher frequencies. The SKA will be the world's largest and most sensitive radio telescope which will have a total collecting area of approximately one square kilometer.

Malaysia would like to become a part of this advance project to drive radio astronomical research in Malaysia to the front line. In fact, Malaysia is the best location that linked Australia and China for better resolution and wider sky coverage.

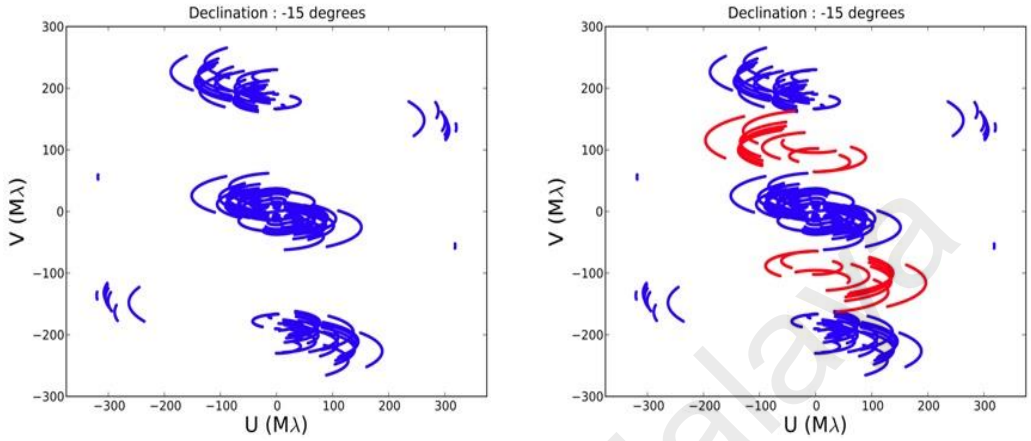

Figure 2.4 The difference sky-coverage area enclosed by the telescope without (left panel) and with (right panel) the involvement of Malaysia that linked Australia and China for better resolution (Image credit: Talk by Prof. Steven Tingay, Curtin Institute for Radio Astronomy)

2.2 Clusters of Galaxies

Scientists throughout the globe agreed that clusters of galaxies are the largest virialized system bounded together by mutual gravitational potential of individual galaxies. They consist of several galaxies or even thousands of galaxies, depends on the richness of the clusters, more commonly followed Abell classification of galaxy cluster. The Abell catalogue was published by George O. Abell in 1958. There were 2,712 rich clusters catalogued in the original version published in 1958. However, it had been added up to 4,073 rich clusters of nominal redshifts below than 0.2, provided by surveys extending from Northern Survey (in 1958) and Southern Survey (in 1989). Table 2.1 shows six richness groups of Abell clusters based on the number of galaxies that

contains in the cluster. The determination of number of galaxies was based on the third brightness member in the cluster (m_3) and should lie between m_3 to $m_3 + 2$.

Table 2.1 Richness group of rich clusters catalogued by Abell

Richness group	**Number of galaxies (N_G)**
Group 0	30 – 49 galaxies
Group 1	50 – 79 galaxies
Group 2	80 – 129 galaxies
Group 3	130 – 199 galaxies
Group 4	200 – 299 galaxies
Group 6	more than 299 galaxies

According to Abell classification, clusters of galaxies can also be divided into two classes, i.e. regular and irregular cluster which differs significantly in their population composition. Regular clusters contain about 70 – 80% percent of elliptical (E) and lenticular (S0's) galaxies. While majority of galaxies in irregular galaxies, more than 50% are spirals in shape. A regular and irregular cluster also differs in galaxy density towards the center and geometrical shape. Regular cluster has a galaxy precisely at the centre of it, while the other galaxies distribute evenly throughout the field, but not for irregular cluster – it shows no significant centre and other galaxies distribute diffusely. In terms of velocity dispersion, regular cluster has higher magnitude compared to that of irregular cluster, which has low velocity dispersion. Examples of regular clusters are Coma, Perseus and A85, whilst for irregular clusters are Virgo, Centaurus and A1689 (Figure 2.5).

Generally, Abell used physical features in determining cluster classification as follow: galaxy population, distance, brightness of the members in the cluster,

distribution of morphological types of galaxy and velocity dispersion. In addition, he also used some other characteristics in cataloging clusters such as distance and mass of the cluster.

Figure 2.5 The example of regular and irregular cluster. Regular Coma cluster is shown in the left panel, while irregular cluster, A1689 is shown in the right panel. Note that the difference in colour is due to the clusters was observed in different portion of electromagnetic spectrum

Clusters of galaxies also can be classified as young or old cluster. The characteristics of young and old clusters of galaxies differ from each other from spirals fractions in the cluster, X-ray temperature, velocity dispersion and galaxy distribution. Based on X-ray observations, the clusters with high spiral fractions (spiral dominating, almost 75% are spirals (Bertram et al., 2006 & Kalloglyan, 1971)), low X-ray temperature, low velocity dispersion and irregular galaxy distribution are classified as a young cluster system. Thus, young cluster usually undergoes ongoing merging process towards the centre of the cluster by the attraction of grandeur gravitational potential well. This shows young cluster is not yet in dynamically relaxed state compare to old cluster which has long dynamical history and hence at the stage of virialized.

Clusters of galaxies are an ideal laboratory to study the formation and evolution of the Universe and also the content of baryonic matter, non-baryonic matter and invisible dark matter that involve in the cosmic evolution. This is due to some reasons proposed by Voit, 2005, which are as follow:

1. The measureable masses in galaxy cluster implied that the galaxy cluster is the largest objects to have undergone gravitational relaxation and entered into virial equilibrium;
2. Clusters are essentially "closed boxes" that retain all their gaseous matter, despite the enormous energy input associated with supernovae and active galactic nuclei, because the gravitational potential wells of clusters are so deep.

Mass of the clusters of galaxies or global mass is an important observable parameter since it is strongly provides the information of the total gravitational effect of individual galaxies within the cluster. The measurable masses of galaxy cluster can be obtained directly by using three independent methods (Bahcall, 1998):

1. Determination of velocity dispersion of the cluster reflects the dynamical cluster mass, within a given radius, by assuming that the cluster is in hydrostatic equilibrium;
2. The hot, X-ray emitting ICM gives the information of temperature and density of the gas that can lead to estimate the global mass, again by assuming the gas obeys the equation of hydrostatic equilibrium;
3. Gravitational lensing distortions of background galaxies can be used to directly measure the intervening cluster mass that cause the distortions.

The mass of clusters of galaxies comes from the contributions of both baryonic and non-baryonic matter. Baryonic matter (which is composed of baryon components such

as proton and neutron) and undetectable dark matter are said to be major building blocks for the structure of the clusters of galaxies. Baryonic matter such as, neutral hydrogen (HI), ionized hydrogen (HII) and helium (He), however contribute small fraction of the total cluster mass, while dark matter enveloped cluster as a huge dark halos, more than 80%. First attempt in quantifying the mass distribution was done by Zwicky in 1930's, by using method of velocity dispersion. Before the discoveries of dark matter, galaxies and the total cluster mass was assumed to share the same distribution (Biviano et al., 2003). Ignoring this assumption, by taking into account the presence of dark matter, can widen significantly the range of allowed cluster's mass (Merrit, 1987).

Since most of the clusters moving at non-relativistic speeds, the dynamics of clusters of galaxies can be treated in Newtonian manner. The application of virial theorem is significantly important because it gives the information of self-gravitating masses that keep the cluster in steady state. This relation states that, the kinetic energy, K is directly proportional to the potential energy, U with constant proportionality – 1/2, by assuming that the moment of inertia, I of the cluster is constant. The use of virial theorem is also important by assuming that the cluster is in hydrostatic equilibrium. This gives rise to the total mass of the cluster as a whole, by considering both visible and invisible stuffs in the cluster. However, before one calculates the total mass using virial theorem (1), the number of galaxies in the cluster should therefore be accounted first by using method of interloper treatment (Wojtak et al., 2007)

The mass of the cluster (regarding the matter distribution in cluster) can be mapped by using various equipment and observed in various waveband i.e. optical, radio, infrared and X-ray. The diversity of different observing method is required since the matter in cluster emits radiation in assorted wavelength. In radio band, for instance, provides the information of HI content in cluster, in which the method has been

implemented in this study. Using radio astronomical technique, also can trace out the behaviour of HI distribution from the cluster centre towards the cluster outskirts. Current estimation of cluster mass, by HI distribution and invisible dark matter, and with corrected today's Hubble constant is about $10^{14} - 10^{15}\ M_{\odot}$ for a typical rich cluster of galaxies (Chapter 1).

As mentioned earlier, clusters of galaxies also contain hot ICM with typical temperature, $T \sim 10^{7} - 10^{8}$ K and luminosities of $L_{\text{X-ray}} \sim 10^{43} - 10^{45}$ ergs/s. Because of its presence, clusters of galaxies show prominent signs of gas depletion due to ram pressure stripping that occurred in dense environment, especially in spirals. It is because, when the galaxies passing through cluster's field at high velocity, they will experience ram pressure on their gas disk and depending on the binding energy of galaxy's own ISM, the ICM will either be forced to flow around the galaxy or will blow through the galaxy, removing some or the entire diffuse ISM. The depletion or stripping of the gas in cluster can cause morphological transformation resulting in the morphological-density relation (Dressler, 1980) and the Butcher-Oemler effect (Butcher & Oemler, 1978). Ram pressure stripping phenomena (first initiated by Gunn & Gott, 1972) is the best candidate to explain the observe event differences between field and cluster spiral in the nearby Universe. This event explains why galaxy morphological type differs at region near the cluster centre and those in the outer region. Spirals near the cluster centre missing a lot of ISM, which is important in stellar formation due to the interaction of ISM-ICM. Thus, it slows down the rate of star formation and tends to transform its spiral shape into lenticulars or ellipticals and could change the colors.

Another important parameter in describing the properties of clusters is mass-to-luminosity ratio (M/L). The luminosity of clusters is determined by defining its appropriate luminosity function, measured of how the objects (galaxies) are grouped by

its corresponding luminosity. More accurately, luminosity function is the number density of galaxies of a specific luminosity in a given volume. The mass and luminosity can be simply related to each other, by taking the ratio of mass and luminosity respectively to produce cluster M/L. In many cluster, the Schechter luminosity function represents a very good fit to the data if the brightest galaxy is regarded in each cluster (Schechter, 1975). For example, in Virgo cluster is exponentially well fitted by the Schechter form. The luminosity function can be unassociated into various kind of luminosity function based on the wavelength band, such that used in this study, $L_{1.42}$, where this luminosity is defined based on hydrogen spectral line emission or radio luminosity. The M/L ratio differs from morphological type of the cluster. M/L ratio appears to flatten and remain approximately constant for rich cluster from scale of ~ 0.2 to at least 1.5 h^{-1} Mpc, gives the value of $M/L \sim 300 \pm 100\ M_{\odot}/L_{\odot}$, as poor cluster gives values of $M/L \sim 200 \pm 50\ M_{\odot}/L_{\odot}$. Kaiser (1998) estimates the value of M/L by using weak gravitational lensing mass estimate of a supercluster of galaxies is about 140 ± 20 $M_{\odot}/L_{\odot}$ which is comparable to that of clusters. Although all the values mentioned above are taken from optical data observed in blue band, it can be used to estimate M/L ratio in radio band. Thus, same conclusion of mass discrepancies in clusters can be made based on radio luminosity and optical luminosity, which is parallel to each other.

2.3 Neutral Hydrogen Mass (M_{HI}) in Cluster of Galaxies

The overall mass of clusters of galaxies can be computed based on the value of integrated HI flux by using HI spectral line observation (Haynes et al., 1997) and can be deduced by applying equation (3). Moreover, the HI mass is distributed diffusely in clusters of galaxies, whether in the galaxy itself or in the field between the galaxies. In a smaller scale of galaxy, measurement of the 21-cm spectral line coming from the ISM that contains HI yields information on the total mass and total hydrogen content of that

particular galaxy. A correlation between these two quantities and morphological type of galaxies have shown that late-type spirals and irregular galaxies in clusters of galaxies are rich in HI meanwhile early-type ellipticals and lenticulars are less in HI (Davies & Lewis, 1973 and Bieging & Bierman, 1977). This means that HI distribution depends on the morphological types of galaxies (Roberts & Haynes, 1994), dispersed at the centre and throughout the field of clusters of galaxies.

The search for HI in the form of ICM was first initiated by Field (1959). The presence of trail galaxies in clusters of galaxies shows that HI gas is being stripped from the galaxies into cluster's field. In Bravo-Alfaro et al. (1997), they show that HI-deficiency is much obvious for spiral galaxies – which rich in HI gas – near to cluster centre because the density of X-ray gas is much higher at the core of the cluster instead of at the outskirt of the cluster. The X-ray gas is said to be responsible for the HI gas to be distributed in the field of the cluster, in the form of intergalactic medium (or IGM) since it stripped away some amount of HI gas in spiral galaxies in ram pressure stripping phenomena – as mentioned in previous section. Typical HI mass of a cluster is about $10^{9–12}$ $M_{\odot}$ (Stroe, Oosterloo, Röttgering et al., 2015). In general, the total HI mass contributes only 8 – 10% of the total mass fraction in clusters of galaxies.

CHAPTER 3 METHODOLOGY

3.1 HI Spectral Line Observation

In this study, the M_{HI} in A262 has been identified by using 7-metre small radio telescope located in Jodrell Bank Observatory (JBO), Manchester, with total collecting area and angular resolution of about 40 m^2 and 0.03', respectively – shown in Figure 3.1. The radio telescope is situated in RQZ area which covered 6 miles in distance. JBO is automatically consulted about any new buildings or developments within the consultation zone as a part of the normal planning permission process. This parabolic dish is capable to identify the M_{HI} in the cluster because of its wider beamwidth. The telescope is equipped with a 21-cm receiver and 5 MHz band sampled by a 64-channel filter bank. The channel of the width is 10 kHz and observation on 21-cm line corresponding to frequency 1.42 GHz i.e. resulting from HI emission, has been used. In the observing room, the signals at frequencies around the HI line are amplified and "mixed" down to "baseband" frequencies between 1 and 5 MHz before entering the spectrometer. The wiring diagram of the telescope is given in Figure 3.2.

All the signals that one deals in radio astronomy are pure random noise. The physical parameter that usually being described for this pure random noise is "noise temperature", measured in Kelvin (K). The total noise power at the output receiver, often called the system noise or system temperature, T_{sys}, can be defined as:

$$T_{sys} = T_{source} + T_{sky} + T_{spill} + T_{rec} \quad (5)$$

where T_{source} is the desired contribution coming from the radio source, T_{sky} is the contribution from the sky around the source, T_{spill} is the contribution from the ground around the telescope and T_{rec} is the noise generated in the receiver electronics. For the observation in this study, the system temperature is about 100 K.

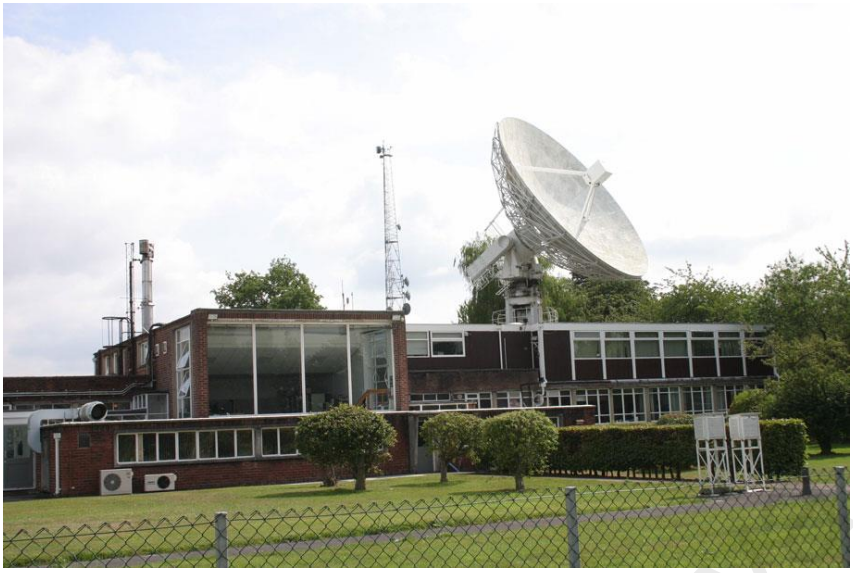

Figure 3.1 The 7-metre radio telescope located in Jodrell Bank Observatory

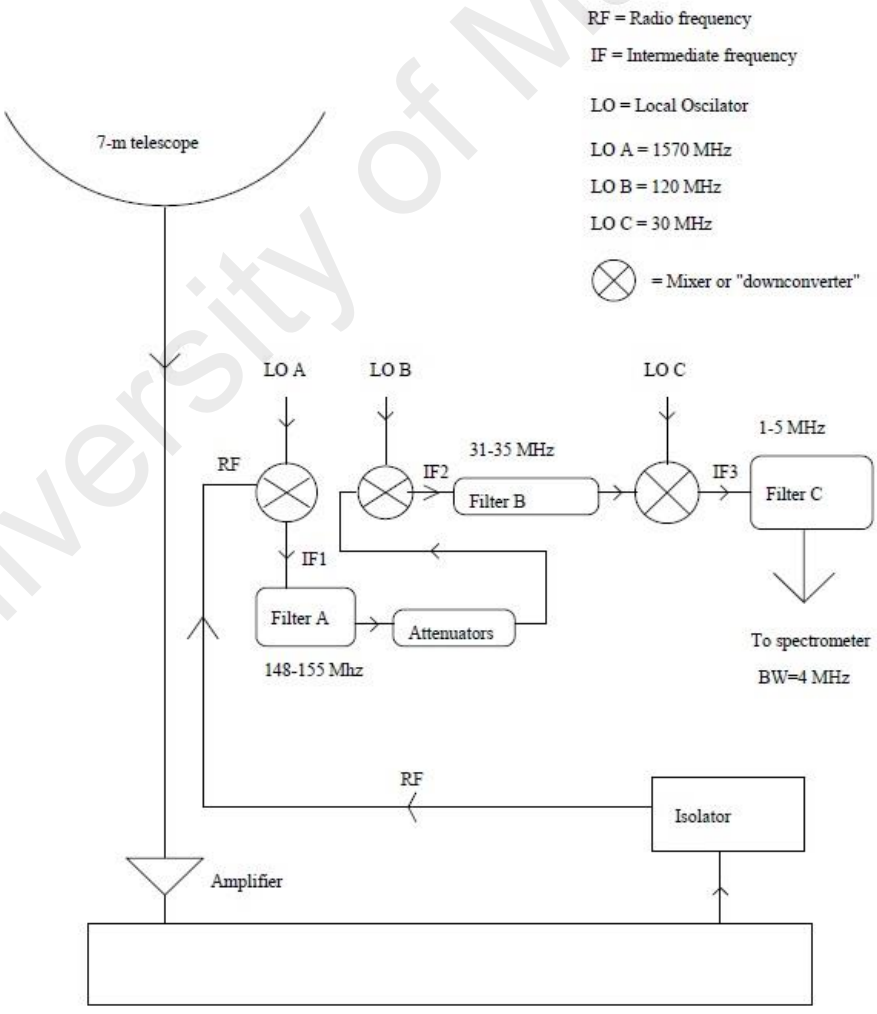

Figure 3.2 The wiring diagram of 7-metre radio telescope

A single observation consists of recording the averaged spectrum for a particular length of time from part of the sky that one interested in. This is called source observation. The raw spectrum appeared when the 'Use Baseline' functions in the GUI display turned off (Figure 3.3). The gain is different at different frequencies across the band at particular range of time – bandpass shape. The curving background produced is just due to the continuum radio emission from the sky plus the receiver noise (right panel of Figure 3.4). Since it is very difficult to find out small changes and a bias in variable gain that we obtained, the standard ways to deal with these problems should be implemented by making a second observation to remove the effects of this bandpass shape. This second observation is called reference observation.

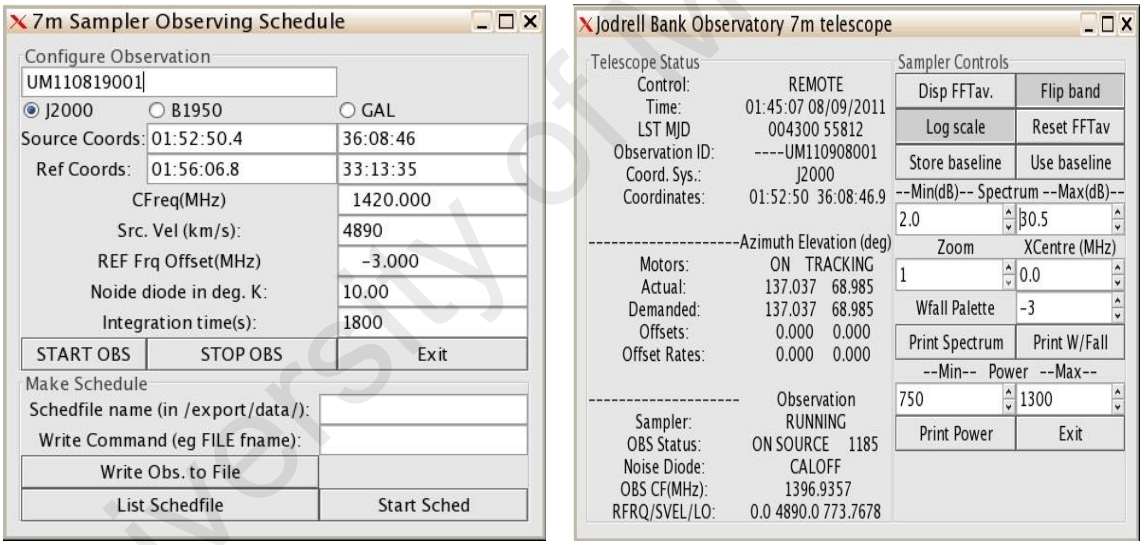

Figure 3.3 The GUI displays of 7 meter radio telescope

Ideally, reference observation should be implemented, where the bandpass shape is the same and includes any other features such as RFI and HI that are not originated from targeted source. It is combined with the source observation and used to normalize the gain across the band so that the gain of each frequency is the same. However, the chosen of reference observation is based on type of targeted object, whether it is intergalactic or extragalactic. There are two types of reference observation:

1. **Frequency switching** – This type of observation usually used for observation of intergalactic objects, such as local HI in the Milky Way, in which the reference has the same coordinates as the source (or object), but the observing frequency is shifted by several MHz. This moves the HI emission outside the band and the reference observation therefore just defines the instrumental response which is then automatically subtracted from the source observation.
2. **Position switching** – This type of observation makes no frequency offset but rather the reference coordinates are shifted by several degrees from the target direction. This observation is vital for extragalactic objects such as other galaxies and clusters of galaxies as it can be used to minimize the contribution of emission from local HI i.e. from the subtraction of HI emission of the target and local HI in the Milky Way.

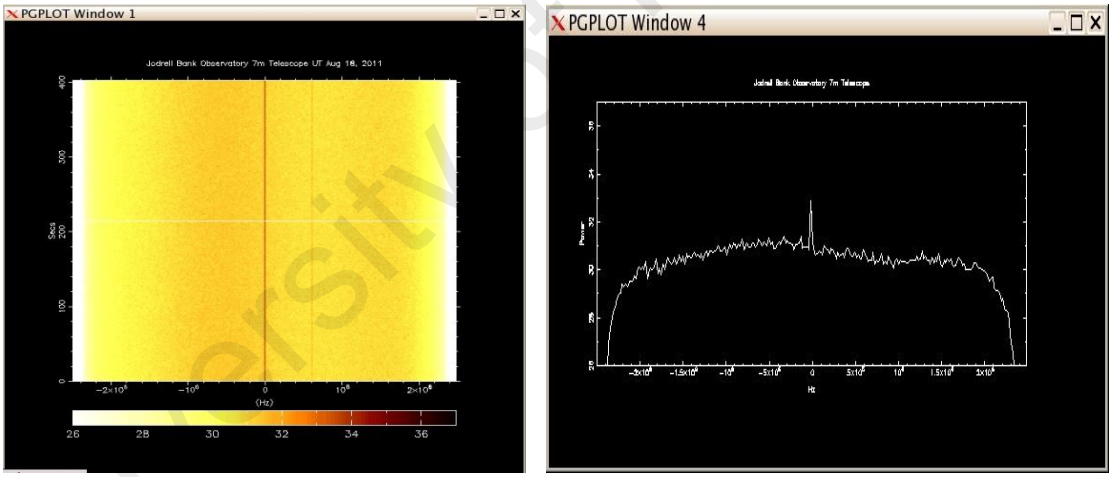

Figure 3.4 The plot windows of 7 meter radio telescope

Since this study used cluster of galaxies as a target, thus position switching for reference observation is necessary. If one happens to look at a source which is not local HI, the observer needs to look at the source and decide on removing everything that does not belong to the source. If the observer changes the frequency, not only might bandpass change, the unwanted signals (from RFI or local HI) will stay in the results. In addition, bringing new RFI or local HI into the band which was not there before will

produce a negative dip in the results. Instead, finding a patch of sky that is away from local HI is vital.

Besides of removing RFI or local HI, the spectrum of extragalactic object should be flattened. If one changes frequency to make a reference spectrum, any RFI and local HI will be left in the band. In addition, if the spectrum is already at an offset frequency due to source velocity, the spectrum will be closed to the edge of the primary filter and so the band shape may be changing with frequency, thus makes the flattening poor. Therefore, the changing or switching in position would be necessary. One should move as short a distance as possible to keep RFI or local HI and ground noise as close as possible, but far enough that there is no source in the reference band. The displays of the band produced can be seen in Figure 3.5 – (a) Source observation normalised with a reference observation at +3MHz. The local HI still exist in the band. (b) Source observation normalised with a reference observation made by moving the telescope about 5 degrees (position switching). Local HI has nearly been removed and the band is flatter compared to (a).

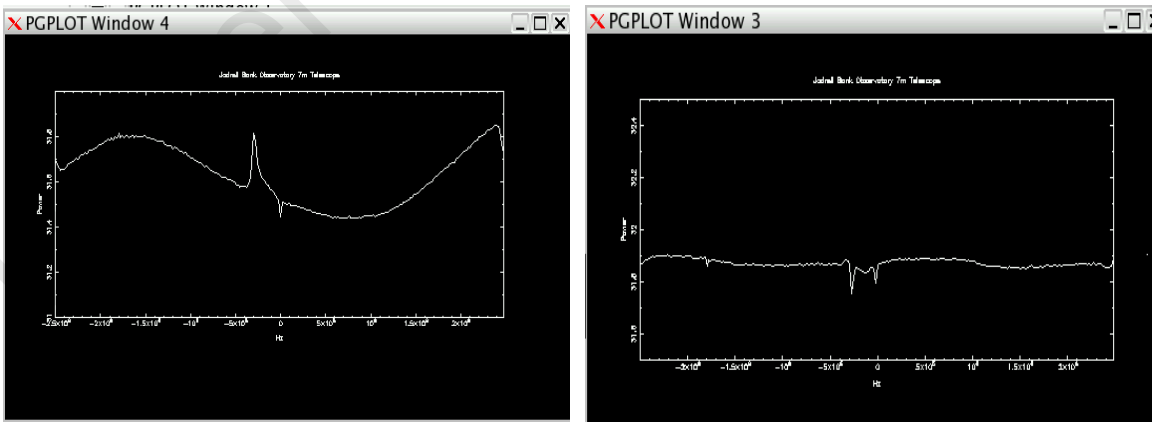

(a) (b)

Figure 3.5 The displays of different mode of observations between (a) frequency and (b) position switchings for extragalactic observation

3.2 Concept of Observation

According to Battye et al. 2004, the synthesized beam size produced by the telescope depends on the collecting area (or size) of the telescope, allowed one to attain M_{HI} for the cluster covered by the beam pattern produced by the telescope. This method can be used to investigate M_{HI} in cluster as a whole, instead of M_{HI} for the individual galaxies in the cluster, in which makes use of much bigger telescope to increase the sensitivity. Hence, smaller dishes give bigger instantaneous FOV, Ω_{inst} and full-width half maximum of synthesized beam size, θ_{FWHM}. In addition, the relation between parabolic antenna beamwidth and its diameter is given by $\theta_{FWHM} = k\lambda/D$, where λ is the wavelength and k is the proportionality constant. This means that the value of θ_{FWHM} is inversely proportional to the diameter of the telescope or in other words, one should use small radio telescope to observe larger objects in the sky. The value of k for the telescope varies about $1 < k < 1.4$, which corresponds to $112.8' < \theta_{FWHM} < 157.8'$. θ_{FWHM} also can be directly obtained from the observation of certain objects in the sky (Chapter 4).

There is also a relationship between θ_{FWHM}, redshift, z, and virialized mass of the object. For three different types of object with masses of 10^{13} $M_{\odot}$, 10^{14} $M_{\odot}$ and 10^{15} $M_{\odot}$, the trend of θ_{FWHM} and redshift shows exponential decrement pattern. In addition, the total collecting area of the telescope should be increased if one wants to observe an object with high redshift. It means that object with low mass requires lower value of θ_{FWHM} and as the value of redshift decreases, one should use a telescope with small total collecting area, and hence with higher beamsize. These trends can be visualised as a plotting of θ_{FWHM} against redshift in Figure 3.6. However, the plot shows only for the case of high redshift objects. The trend for objects of smaller redshift can be portrayed as in the zoomed-in plot of Figure 3.6. It is clearly shown that, in Figure 3.7, the nearly

straight line trend provides a lower limit of θ_{FWHM} that should be accounted for objects of lower redshift.

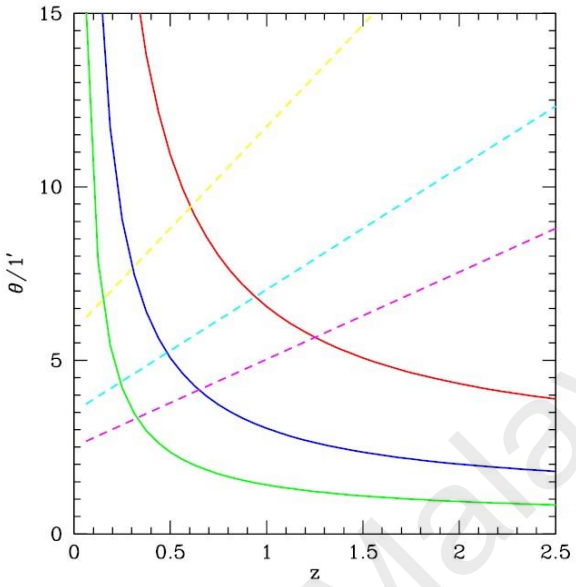

Figure 3.6 The variation angular diameter size with the total virialized mass of the cluster, represented by green, blue and red solid lines for M_{vir} = 10^{15} $M_{\odot}$; 10^{14} $M_{\odot}$ and 10^{13} $M_{\odot}$, respectively. The dashed lines stand for estimated synthesized beam size for three different configurations or accumulated area, A (top, A = 5000 m^2; middle, A = 10000 m^2; bottom, A = 15000 m^2) (Image Credit: Battye et al., 2004)

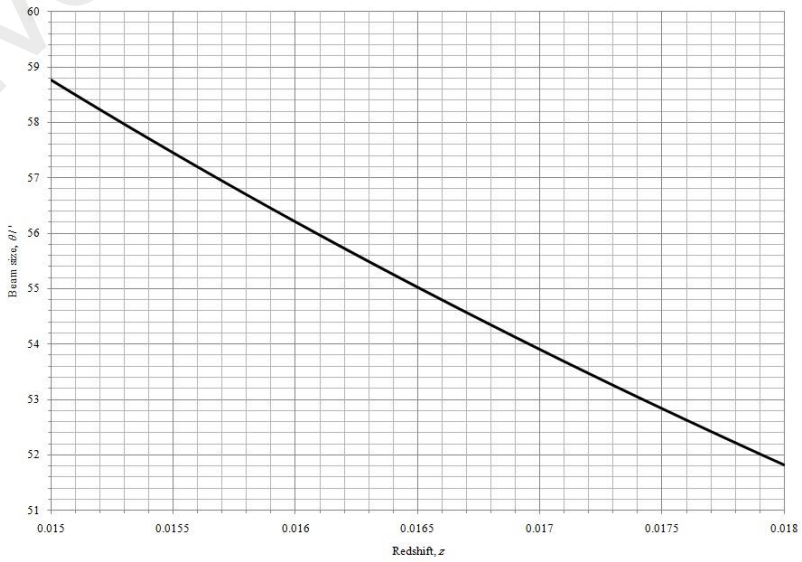

Figure 3.7 The zoomed-in graph of Figure 3.6, for low redshifts object

The period of the observation to take place is depending on sensitivity of the instrument used. Improvements in receiver stability and the increased use of correlation spectrometers have allowed more frequent use of longer integration times required to observe weak spectral line observations lasting several hours are quite common (Rec. ITU RA.769-2). It took several months to accumulate the observational data to be integrated for the work. The observation period are divided into three phases i.e. August 2011 – January 2012, November 2012 and December 2012 – January 2013, with total integration hours of approximately 370 hours. The observational period was determined based on the availability of the telescope and location of the source (the rising and setting time of the source had to be considered). It is necessary to have longer observational period. The sensitivity of the instrument S_v, in terms of antenna system temperature, T_{sys}, for a single dish antenna can be represented as follow:

$$\Delta S_v = 2k[t\Delta v]^{-1/2}[\frac{T_{\mathrm{sys}}}{\mathrm{K}}][\frac{A_{\mathrm{e}}}{\mathrm{m}^2}]^{-1} \tag{6}$$

where k is the Boltzmann constant, A_e is the effective collecting area of a single radio telescope of diameter, D and Δv is frequency bandwidth. According to the equation above, to acquire the minimum rate of change of flux density, the integrated observational period should be increased to several hundred hours in order to amplify the probability of finding possible detection from the source, yielding to better results. Commonly, it takes about 50 – 60 days – which equivalent to 1200 – 1440 hours – observational integration time to accumulate the data into a single final integrated spectrum of targeted source, especially when one deals with less sensitive instrument.

The HI mass is related to the integrated 21-cm flux over the velocity distribution. For an unresolved source, the flux density S_v is related to the antenna temperature, T_{A} with

$$S_\nu = \frac{kT_A}{A_e} \tag{7}$$

where k is Boltzmann constant, A_e is the effective area. The effective area Ae is related to the geometric area $A_g = \pi D^2/4$ with $A_e = \eta A_g$, where η is the telescope efficiency. The A_e of 7-metre radio telescope is calculated to be about 1.77×10^5 cm^2. On the other hand, if the HI is a resolved source i.e. uniformly distributed over the field of view of the telescope, then the HI flux density is related to the brightness temperature with the equation

$$[\frac{S_\nu}{\text{Jy}}] = 2.65[\frac{T_B}{\text{K}}][\frac{\lambda}{\text{cm}}]^{-2}[\frac{\theta_0}{\text{arcmin}}]^2 \tag{8}$$

where λ is the observing wavelength in unit of centimeters and θ_0 is the main beam of the telescope in arc minutes. Then, the HI mass can be computed by using equation (4) in Chapter 1.

3.3 Candidate's Selection

There were a few candidates have been listed for the work, as shown in Table 3.1. However, A262 has been chosen as an object of study. The chosen of A262 is based on certain criterion that fit with the purpose of the study i.e. to use small radio telescope to determine the value of hydrogen content in a nearby cluster of galaxies as a whole. The criterions that have been considered are as follow:

(a) the object should have relatively small value of redshift,

(b) the object is located at Northern Hemisphere,

(c) the object should confine within the beam size of the telescope, and

(d) the object has higher fraction of spirals that could be used to probe the location of HI gas.

Table 3.1 The candidates being considered in this study

Cluster	RA (h m s)	Dec (' ")	Redshift (*z*)	Velocity (km/s)
A85	00 41 37.8	-09 20 33	0.0551	16507
A119	00 56 21.4	-01 15 47	0.0442	13251
A262	**01 52 50.4**	**+36 08 46**	**0.0163**	**4890**
A373	03 38 30.0	-35 27 18	0.0046	1380
A1060	10 36 51.3	-27 31 35	0.0114	3420
A1367	11 44 44.6	+19 41 59	0.0216	6480
A1656	12 59 48.7	+27 58 50	0.0231	6930
A1689	12 26 32.1	+12 43 24	0.0038	1140

A262 is one of the largest clusters in Pisces-Perseus Supercluster (PPS) (located nearby to group of galaxies N383 and N507) and classified as irregular cluster since it has irregular shape and low central galaxy, but high central gas density. The accumulated mass of the cluster reach up to 10^{14} $M_{\odot}$. It is a part of Local Group Supercluster with its coordinate given by RA = 01h 52m 50.4s and Dec = +36° 08' 46" with redshift of z = 0.0163 (Struble & Rood, 1999) and v = 4890 km/s. It has been noticed that A262 categorized as *cD* (cluster dominant) galaxy cluster with its centre NGC 708, a subtype of type-D giant elliptical galaxy (Bertram et al., 2006) and also strongly X-ray emitting source (Bîrzan et al., 2004). A262 is located approximately at D = 69 Mpc (luminosity distance) relative to the Earth. A262 exhibits the viriliazed mass, M_{VT} and mass-to-luminosity, M/L ratio that are typical of rich clusters, even though A262 is classified as intermediate richness cluster, based on the number of galaxies in the cluster. However, according to Abell, A262 falls into richness class 0 because at least 40 galaxies in A262 have not more than 2 magnitudes fainter than the third brightest member. The size of the cluster is 211 arcmin (about 4.45 Mpc) in diameter, as retrieved from a database.

Velocity dispersion of A262 is relatively low (about 500 km/s) compared to Coma or Virgo cluster which values lie in the range of 700 – 1000 km/s. It has mean velocity

within less than 0.5° from the cluster centre of about 4839 ± 89 km/s, with $M_{VT} = 0.6 \times 10^{14} h^{-1} M_{\odot}$ and mass-to-luminosity ratio, $M/L = 389$ ($M_{\odot}/L_{\odot}$) and mean velocity within less than 1.4° is 4903 ± 71 km/s which coincide with the radial velocity of NGC708, v = 4898 km/s (Sakai et al., 1994). Based on velocity dispersion profiles, A262 shows a trend in such a way that the velocity dispersion is decreasing from the centre to the edge of the cluster and the same trend goes for mean velocity. However, at a certain radius, mean velocity and velocity dispersion is slightly higher. The different value of velocity dispersion, however, affects the estimation of M_{VT} in A262 (and all clusters, in general).

A262 is a spiral rich cluster which comprises 75%, both normal (S) and barred spiral (SB) of the galaxies down to magnitude 16.8, while elliptical (E) and lenticular (S0) – both make up only 20% of the total galaxies (Kalloglyan, 1971). Among the spirals, 80% are normal and the rest are barred. In the Vaucoleurs' sample, Sa and Sab type constitute 59% and SB type constitute 37%. The average flux density for spirals, $\langle S_v \rangle_{spirals}$, in A262 is 5.359 Jy km/s, which is higher than the average flux density for other morphological types of galaxies, $\langle S_v \rangle_{others}$, which contributes to 3.254 Jy km/s – obviously shows that spirals are HI-rich galaxies (Giovanelli et al, 1982). Because of high fraction of HI in spirals, they represent higher value of luminosity, L – which agreed with the fact that spirals are among the brightest objects in the Universe.

The distribution of different morphological type of galaxies varies from the cluster centre to the edge of the cluster. As shown in Figure 3.8, most of the spirals pervade throughout cluster field, while elliptical and lenticular located at highly-populated region at the centre. Hence, elliptical and lenticular tend to be near to the core of the cluster. This distribution is in agreement with galaxy distribution in local Universe, which states that almost 90% of the population in the core region of rich and

intermediate cluster consist of E and S0's, while S's and SB's are dominated throughout the field of the cluster (Dressler, 1980).

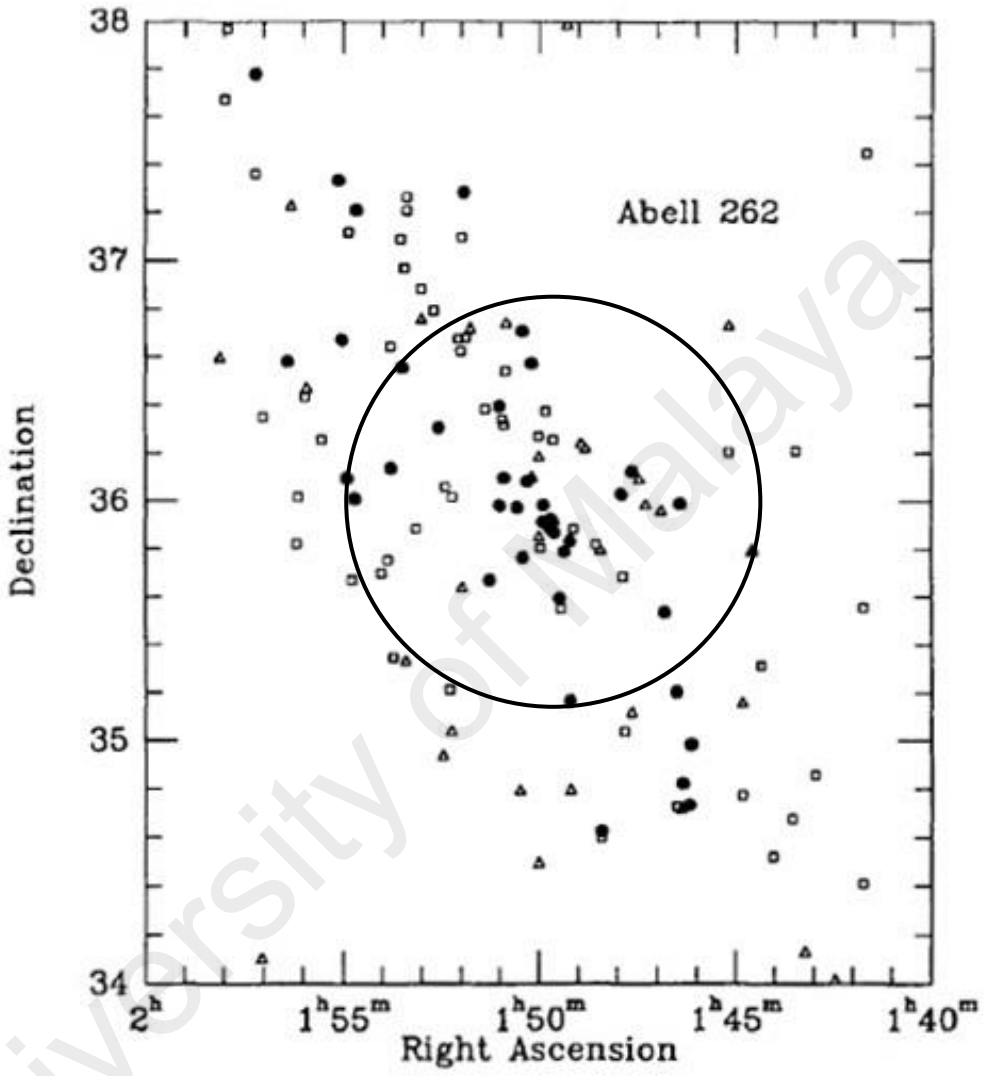

Fig. 3.8 Galaxy spatial distribution according to different morphological types in A262. Note: Filled circle: elliptical and lenticular; square: spirals, triangle; other morphological types, such as dwarfs and irregulars. The black circle represents the approximate area covered by the beamwidth of the telescope (Image credit: Sakai et al., 1994)

The ICM temperature, T_{ICM}, in A262 is about 2.8×10^7 K and its luminosities in different waveband is given by $L_B = (7.4 \pm 0.01) \times 10^{43}$ erg s^{-1} (Bregman, McNamara &

O'Connell, 1990) $L_{1.42}$ = (2.1 ± 0.07) × 10^{39} ergs/s and $L_{X\text{-ray}}$ = (3.07 ± 0.01) × 10^{43} ergs/s (Bîrzan et al., 2004). Jones & Forman (1991) identified that A262 shows typical signs of less evolved system with a stationary dominant at its centre, in other word, A262 is not yet in relaxed state. However, Sakai et al. (1994) suggests that the densely-populated core of A262 is virialized or in equilibrium. Because A262 displays high percentage of spiral, low X-ray temperature (compared to the clusters in its class), low velocity dispersion, classified as irregular galaxy cluster and shows the presence of massive, centrally located galaxy; then, A262 is dynamically a young cluster through the observation in X-ray band (Jones & Forman, 1991) and might undergo merging process.

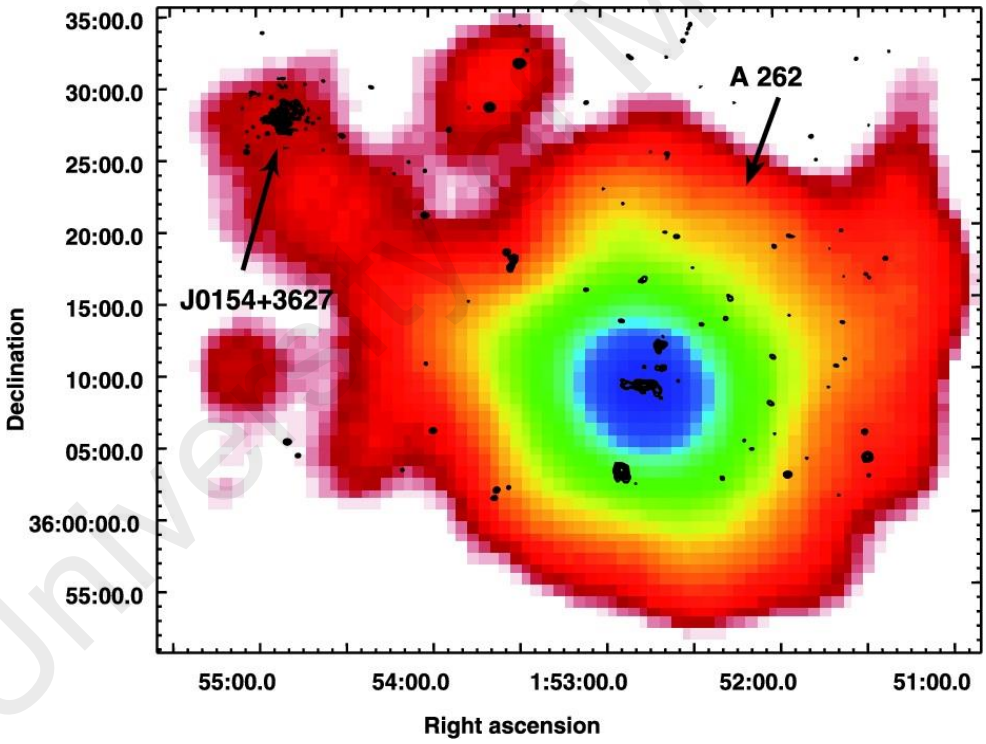

Figure 3.9 The X-ray image of A262 that shows the distribution of hot intracluster medium (Image credit: Bîrzan et al., 2004)

Without exceptional, spiral galaxies members in A262 exhibit ram pressure stripping due to the interaction of ISM within the galaxies and the hot tenuous X-ray emitting

ICM that lies between the galaxies or ISM-ICM interaction. A262 spiral galaxies members are deficient in atomic gas towards the centre i.e. galaxies near the cluster centre stripped more gaseous compared to field galaxies which resemble normal amount of HI (Giovanelli et al. 1982). Since the HI content of individual galaxies depends on the distance from the cluster centre, gas stripping of field galaxies is less effective compared to those near the cluster centre resulting in irregular HI distribution. Phenomenon of ram-pressure stripping leads to morphological-density relation (Dressler, 1980), later to explain why it is the distribution of galaxies varied within a certain radius from the cluster centre.

Bravo-Alfaro et al. (1997) show that, in some individual galaxies the distribution of HI is asymmetrical – signs of ISM-ICM interaction that stripped the gas out from the galaxies. Within the radius of 1° from the cluster centre, it is found that majority of the spiral galaxies to be more extended in the HI than in the optical region. Bravo-Alfaro et al. (1997) also show that the HI distributions of three galaxies in the north east region near to the centre NGC 708 are slightly offset to the west of the optical position. In Giovanelli et al. (1982), more than 80% of the galaxies within the central square degree of the cluster are deficient while only 15% show deficiency in the rest of the field. The HI deficiency of A262 is also correlated to galaxy size.

3.4 Archival Observation

The NASA/IPAC Extragalactic Database (NED) is widely used by astronomers around the world because it contains crucial astronomical information on extragalactic objects such as galaxies, active galactic nuclei (or AGN) and clusters of galaxies. It was established by astronomers George Helou and Barry F. Madore in the late of 1980s. NED contains more than multi millions data ranging from photometric data, redshift and diameter measurements, object's classifications maps as well as journal articles,

notes and abstracts. Thus, this database was chosen based on its powerful data mining and cited for various studies in astronomy.

A compilation of data from NASA/IPAC database has been retrieved and analyzed in particular aspect according to the significant of the study. The important of archival observation is to determine the number of galaxies bounded by a given radius. Clusters of galaxies perhaps contain of galaxies that are not bound in its gravitational potential well. These galaxies are considered as an interloper, since they do not contribute to the gravitational effect of the cluster. Such interlopers should be removed statistically by using any type of method in order to modeling cluster's dynamics. The method of interloper's removal can be divided into two types i.e. direct and indirect methods.

Several techniques have been used for direct method in attempting to remove the interlopers, for example, by evaluating the line-of-sight velocity dispersion of the galaxy sample, σ_{los} and iteratively eliminate outliers with velocities larger than $3\sigma_{los}$ – in which the technique has been used throughout this study. The technique was proposed by Yahil & Vidal (1977) by using the properties of line-of-sight velocity distribution of the galaxies in the cluster that exhibits nearly to a Gaussian fitting. Wojtak et al. (2008) used direct method and found that about 60 – 70% outliers can be removed with low contamination of the sample of about 2 – 4%. He also used indirect method in comparison with direct method. The information of the numbers of outliers that should be removed is vital in reducing the changes in mass estimator (Perea et al., 1990). This would allow one to determine the exact number of members in the cluster leads to evaluation of gravitational mass that keep all the members without flying apart. Additionally, the determination of true cluster member provides the evidence of substructures in clusters of galaxies. For example, 143 galaxies were found to fall

within z = 0.044 and 0.068 in galaxy cluster A3667 and showed it was a system merging in the plane of the sky (Johnston-Hollitt et al., 2008b).

The distribution of line-of-sight velocity of the galaxies within a certain range of radius has been presented in this study. The chosen of the radius is based on the radius that can be enveloped by the beam size of the telescope. As mentioned in the last paragraph, removing the non-members of the cluster in determining the total mass of the cluster or M_{VT} is vital. Thus, direct method of removing the outliers has been implemented in this study since it shows significantly good tracer of mass estimator (Wojtak et al., 2008) – this also lead to a cluster boundary (or cluster member) for spectroscopic analysis.

NED is also useful in providing photometric data for the total stellar mass (ΣM_i) and virialized mass (M_{VT}) calculations. The apparent magnitude from the Two Micron All Sky Survey (2MASS), represented by K_s, is required to estimate the total stellar mass of A262. The estimation also should confine into the number of galaxies present within the FOV of the telescope and within the velocity range of the cluster obtained from HI spectral analysis. To find the stellar mass of individual galaxy, one should use formula that relates K_s data and absolute magnitude of the galaxy, M_K, as stated below (Yen-Ting Lin et al., 2003):

$$M_K = K_s - 25 - 5 \log (d_L) - A \tag{9}$$

where d_L is the luminosity distance in Mpc and A is the galactic extinction. The value of M_i of each individual galaxy can be found by using relationship involving M_K and the luminosity of the galaxy, L_{galaxy}. The relationship is then given by:

$$\frac{L_{galaxy}}{L_\odot} = 10^{(M_K + 3.39)/2.5} \tag{10}$$

where 3.39 is the absolute *K* magnitude of the solar luminosity. The galaxy *K*-band stellar mass-to-light ratio is about 0.7 of the solar *K*-band mass-to-light ratio. The final stellar mass of the galaxy, in terms of solar mass, should be multiplied by a factor of 0.7. Hence, the relation between the luminosity and mass of the galaxy is given by equation below:

$$M_i = M_{\text{galaxy}} = 0.7 \frac{L_{\text{galaxy}}}{L_{\odot}} \tag{11}$$

where M_i (or M_{galaxy}) is the mass of the galaxy and L_{galaxy} is its luminosity. Thus, the total stellar mass can be computed by summing up stellar mass of all individual galaxies in the cluster, denoted as ΣM_i

The virialized mass, however, made use of velocity dispersion analysis, which also depends on the number of galaxies within a given radius and velocity range. In this case, the information about velocity of individual galaxy is significantly important. By applying equation (1), the estimation value of virialized mass can be computed straightforwardly.

CHAPTER 4 RESULTS AND DATA REDUCTION

4.1 Data Compilation

This section can be separated into two groups of data: observational data (obtained from observations) and archival data (obtained from NED database).

The observational data needs to be analyzed to produce possible detection of the source. All the raw spectra should passing through few important steps in analysis i.e. baseline fitting, spikes removal and finally, staking in order to come out with triangle-shaped spectrum near to the cluster velocity which resembles the possible detection from the cluster. However, a spectrum that shows a clear detection of A262 should be corrected to a few factors such as correction on a velocity with respect to local standard of rest, V_{LSR}, precession, aberration and recession, before these spectra come into stacking process. The results from the observation will be discussed in Sec. 4.2.

The importance of archival data is to provide the information of how many members of galaxies that belongs to A262 and confined in a boundary given. In this analysis, the exact number of galaxies that is confined in the gravitational potential well of the cluster was determined appropriately. This is called spectroscopic analysis which using optical data of the individual galaxies within a certain range of radius. A term called interloper – also known as outliers – defined as a non-member of the cluster that should be removed to reduce bias in mass estimation of the cluster. Wojtak et al. (2008) introduced two methods of interloper removal, i.e. direct and indirect methods. However, direct method has been chosen for this study due to its low contamination in the sample. Sec. 4.3 provides the outcome of such analysis in determining a non-member of A262 – if there is any.

4.2 Observational Data

A long series of observation has been carried out to perform best results. The observation includes (1) the determination of beam size of the telescope, (2) observation on the standard sky region for HI observation and (3) observation on A262.

4.2.1 Determination of Beam Size of the Telescope

Before the initiation of the observation on the galaxy cluster, one should calibrate the instrument by tracking the telescope to a certain region in the sky. Cygnus A (or Cyg A) has been chosen for the calibration of the telescope since it strongly emits radio emission in the sky, located in the constellation of Cygnus. From the calibration of this bright astronomical radio signal, the value of half-power beamwidth (HPBW) or full width of the beam at the half power has been determined, directly calculated from the spectrum of Cygnus A. This value provides the information of the degree of the main beam pattern of the telescope – the region of sky to which a radio telescope is sensitive to detect a source.

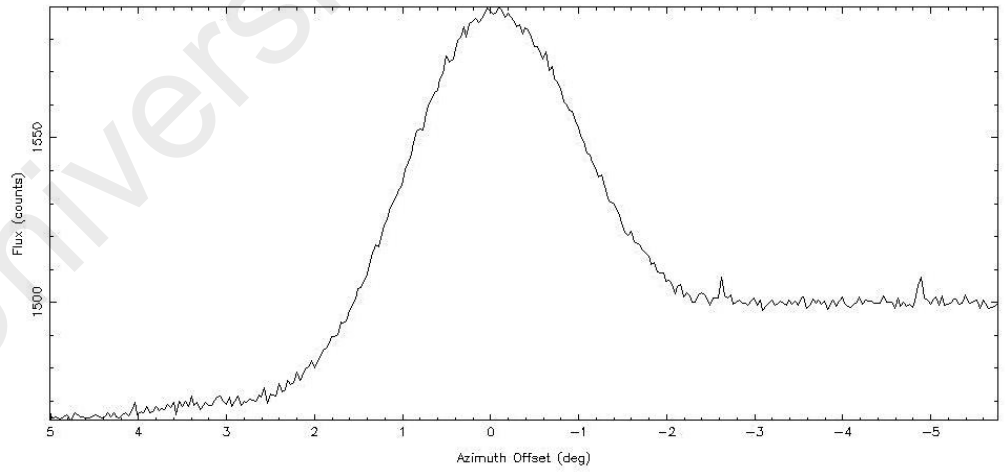

Figure 4.1 The spectrum of Cygnus A obtained from the observation

Furthermore, the value of power radiated by the source has been estimated, by proportion of the noise diode's temperature (10 °K) which is switched on for a few

seconds after scanning across the source is completed. The total time taken for this calibration to take place is about 150 seconds. For 7-metre radio telescope, the θ_{FWHM} produced is about 2.3°, which is equivalent to 138 arcmin (the radius of the cluster bounded by the telescope, R = 69 arcmin). The actual diameter of A262 is about 211 arcmin. Thus, the telescope covered almost 65% of the cluster's area and the determination of M_{HI} was restricted to this boundary only. Since the area of the cluster confined within the θ_{FWHM}, the cluster is then quantified as resolved source. Thus, the evaluation of M_{HI} of A262 should be based on the S_v value obtained by using equation (8).

4.2.2 Source Calibration by Using S7 Sky Region

Besides the determination of θ_{FWHM} of the telescope, the source calibration on standard region should be carried out before further observation on A262. There are four regions used as a standard region in 21-cm observation, recommended by International Astronomical Union (IAU) i.e. S6 (l = 1.91;b = 41:42), S7 (l = 132°, b = –1°), S8 (l = 207°, b = –15°) and S9 (l = 356°, b = –4°). However, in this study, S7 sky region has been chosen for HI calibration. The uses of standard regions are to: (i) permit the brightness temperature scales of HI surveys to be intercompared, (ii) provide easy way of checking the internal calibration of the equipments; and (iii) provide a means of calibrating an antenna-receiver system (Williams, 1973).

The RMS error in the calibration of S7 that should be applied to the measurements on A262 has to be considered. There are two cases in deciding on the necessity of the source calibration, either single long run on S7 or run on S7 before and after the observation on A262. If the system seems stable, perhaps a single long run on S7 would be as effective as several short ones. If there is a lot of variation in the S7 values, one may need to do run before and after the observation on A262. The observation on A262

was commenced when the decision whether source calibration had to be made or otherwise.

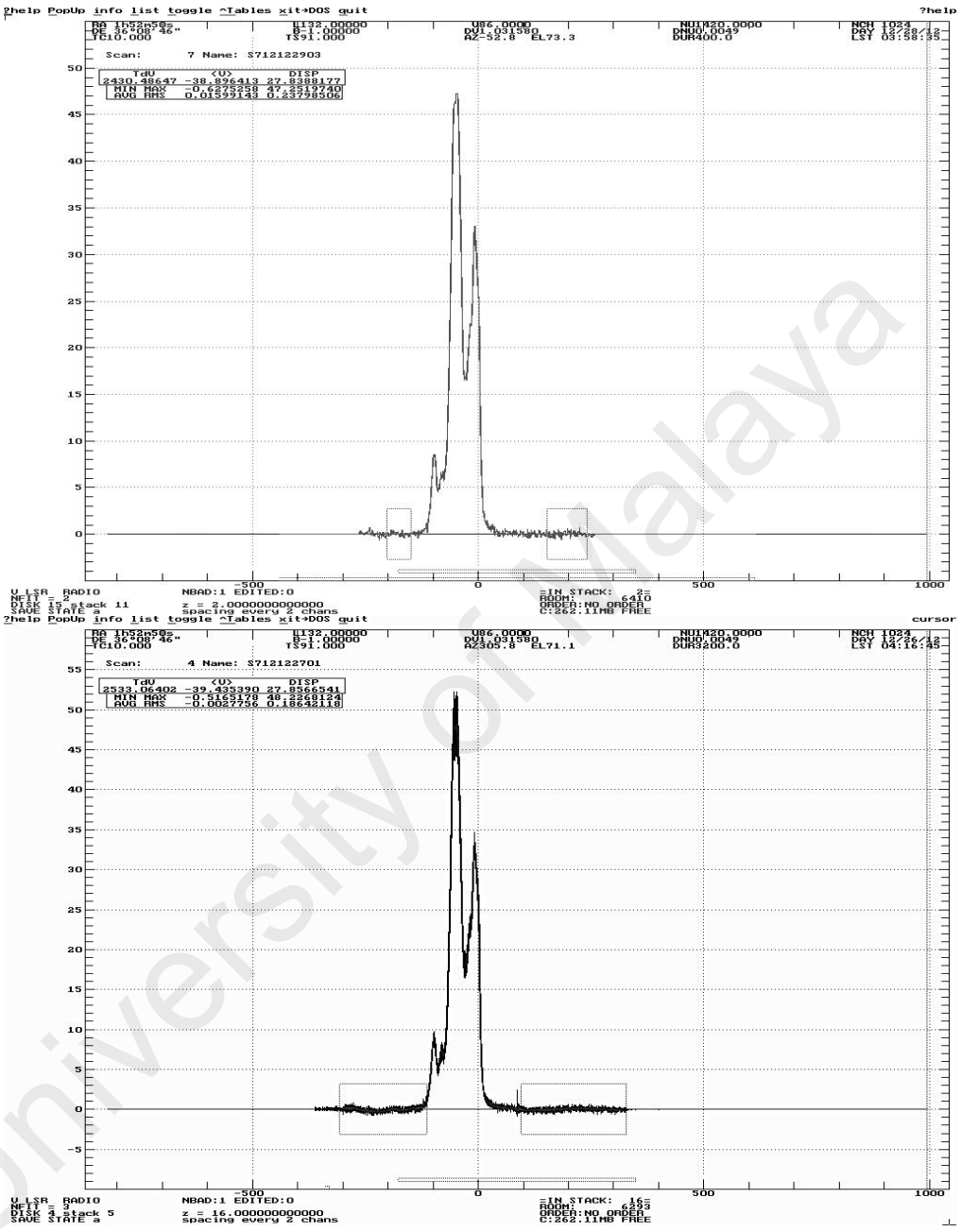

Figure 4.2 Top: A sample of S7 observation. According to a few scan on S7, the value of the flux seems stable from one to another – even though there is a tiny difference between those scans. Thus, single long run on S7 has been chosen before the observation on A262 commenced. Bottom: The integrated spectrum of S7. The

spectrum peaked at about 48 counts. The value of $T\ dv$ was then compared with reference value from Kalberla, 1982

Williams (1973) worked out on S7 study for standard region in 21-cm line observation, including three others, and obtained the profile for S7 region as well as its contour maps. Using a range velocity without including the range of local hydrogen, the experimental brightness temperature of S7 was measured. For each observation, a set of S7 calibration is required since comparing the proportion value in flux density to the brightness integral of S7 allowed us to calculate the flux density radiated by the candidate.

The spectra of S7 should be integrated to obtain the average value. This average value used for the comparison with the theoretical value from previous studies. The value from Kalberla, 1982, with $T\ dv$ = 4600 °K km/s, has been chosen to be intercompared with S7 observation in this study. The temperature integral from the observation of S7 is about 2533 °K km/s. These values can be used to find temperature scaling of HI mass for A262. The proportion value that should be used to scale the temperature for the spectrum is about $(T\ dv)_{obs}/(T\ dv)_{ref}$ = 0.5507, where $(T\ dv)_{obs}$ is the temperature integral from observation, while $(T\ dv)_{ref}$ is the temperature integral from Kalberla, 1982. This value is then being multiplied by each spectrum of A262 for *y*-scaling.

4.2.3 Observation on A262

The raw spectrum of A262 has been obtained short after the observation on A262 (with different duration) was done. The spectrum was stored in the form of ASCII file, one of the text file formats that consist of ASCII characters. Then, the file had to be converted into binary file (FITS file) by using DOSBox, emulator software that imitates similar functions of a primary computer system in a different secondary system. The

format conversion is necessary in order to step on to analyzing process of the data i.e. baseline fitting, spikes removal and stacking. Longer integration time is required (as mentioned in Chapter 3) to have better quality of final result.

The name of the files of observation is listed in Appendix A. The total number of observations is 213, yielding to 368.29 overall hours of observations – or about 15 days. The table shows some vital parameters, i.e. date of observation, local sidereal time (or time of observation), the azimuth and elevation of the telescope as well as the duration of the observation. Figure 4.3 shows the frequency of different observation period on A262. The longest duration is about 10 800 seconds and the shortest one is 120 seconds. However, duration of 7200 seconds has the highest frequency.

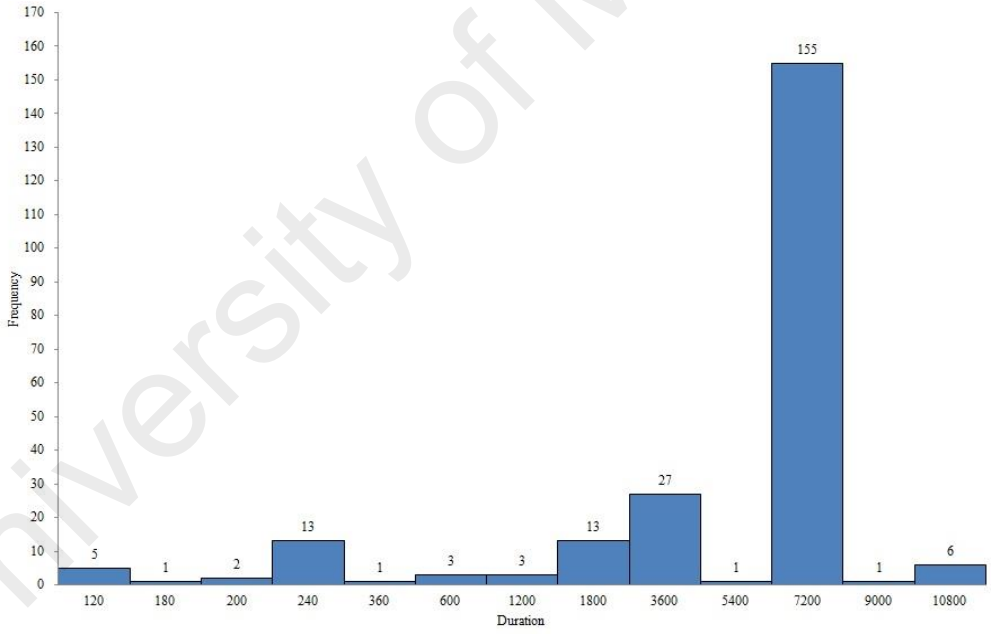

Figure 4.3 The histogram of the duration versus frequency. 7200 seconds of observation has the highest frequency

4.2.4 A262 Raw Spectrum

There are 231 spectra of A262 have been obtained from the observations (the table of 231 sets of observation is shown in Appendix A). For each set of observation, the raw spectrum was produced by the telescope once the observation has completed. However, the shape of the spectrum could be different when the reference frequency offset set to be 0 or –3 MHz. The spectrum produced shows the variation of flux (arbitrary unit), with its corresponding velocity, measured in km/s. DRAWSpec software was used for analysis process. Some important commands in DRAWSpec that had to be used while doing the analysis are mentioned in Appendix C. Each spectrum must go through the process of polynomials baseline fitting and spikes removal due to either internal or external interference, before being stacked. Some of the spectra show smooth polynomials curve with the present of some emission and absorption lines (or RFI).

The range of the velocity is about 4434 km/s to 5494 km/s. In some cases, the spectrum produced a spike in absorption line near to the source velocity i.e. 4976 km/s. Some of the spectra also show no significant detection from A262 and should be omitted from the subsequent stage of analysis. The range of the flux varies from one observation to another. Figure 4.4 shows several raw spectra that might show significant signal from the source. Before further analysis, the determination of spectrum that should be accounted for in the next stage of analysis had to be precisely verified. If there is no signal at all near to the source velocity, the spectrum had to be neglected. Some of the spectra that show possible detection from A262 are shown in Figure 4.4.

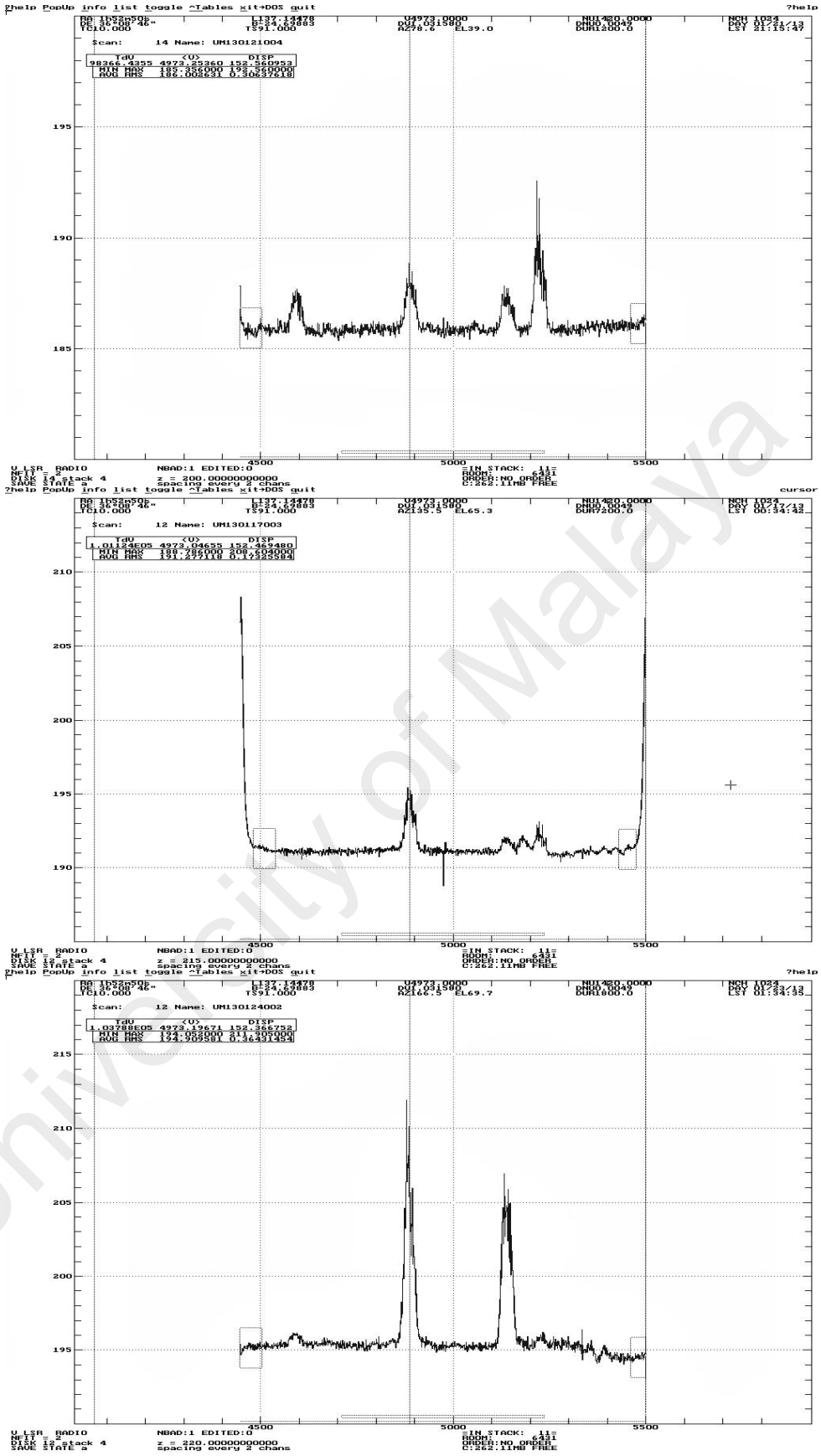

Figure 4.4 Spectra that show significant peak near source velocity

4.2.5 A262 Data Reduction

There are several spectra have been identified that show a detection from A262. These spectra were being analyzed and reduced. Table 4.1 shows the list of the reduced spectra of A262 to be stacked in the final stage of analysis. The total number of observation that shows detection from the targeted source is only about 19 observations and the rest can be considered as unsuccessful observation since they showed no prominent sign of detection. The 19 possible spectra of cluster A262 obtained from the observation are shown in Appendix B.

Table 4.1 The list of chosen spectrum for further analysis of stacking

Name of files (cont.)	Name of files (cont.)
UM110823001	UM121102005
UM110825002	UM121103002
UM110826002	UM121103003
UM111223003	UM121103004
UM111223004	UM121104003
UM111226004	UM121104005 (I)
UM111226005	UM121104005 (II)
UM111227001	UM121229001
UM111227002	UM121230001
UM121102004	

The chosen of 19 observations for stacking analysis is due to they obviously shown prominent signs of the target based on the peak appeared near to source velocity after baseline fitting and spikes removal analysis. Despite relatively large number of observations, only a few of them had be taken into account for stacking analysis, as the observation might result to some degree of difficulties primarily because of the sensitivity of the telescope used in this study. These spectra were then being stacked to produce a final integrated spectrum. The spectrum is shown in Figure 4.5. The final binning of final integrated spectrum with error bars is shown in Figure 4.6. The spectrum in Figure 4.6 is well-fitted with Gaussian distribution with peak velocity of about (4970 ± 0.53) km/s, only about 0.12% more than reference value.

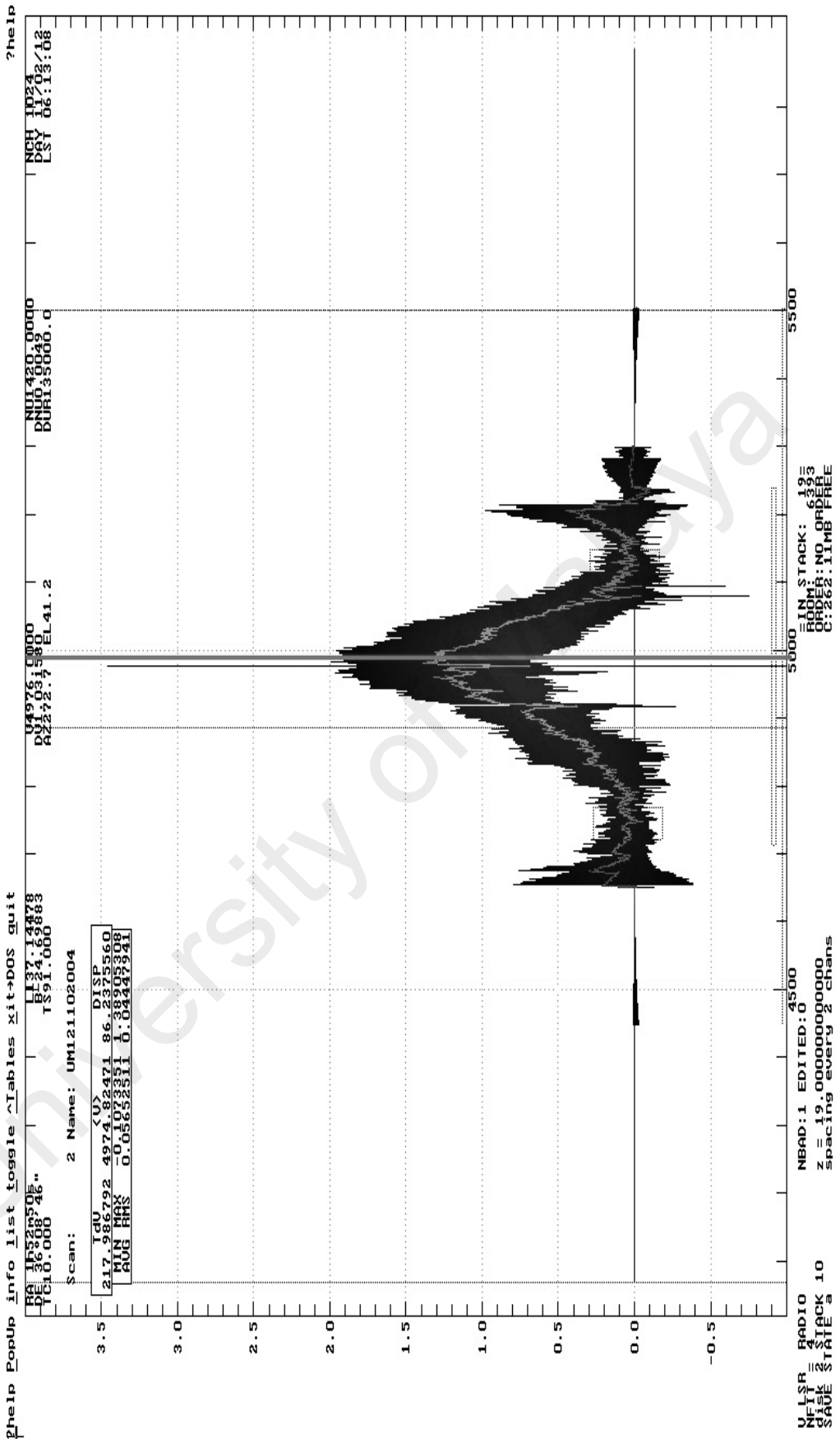

Figure 4.5 The final integrated spectrum of A262 from 19 spectra

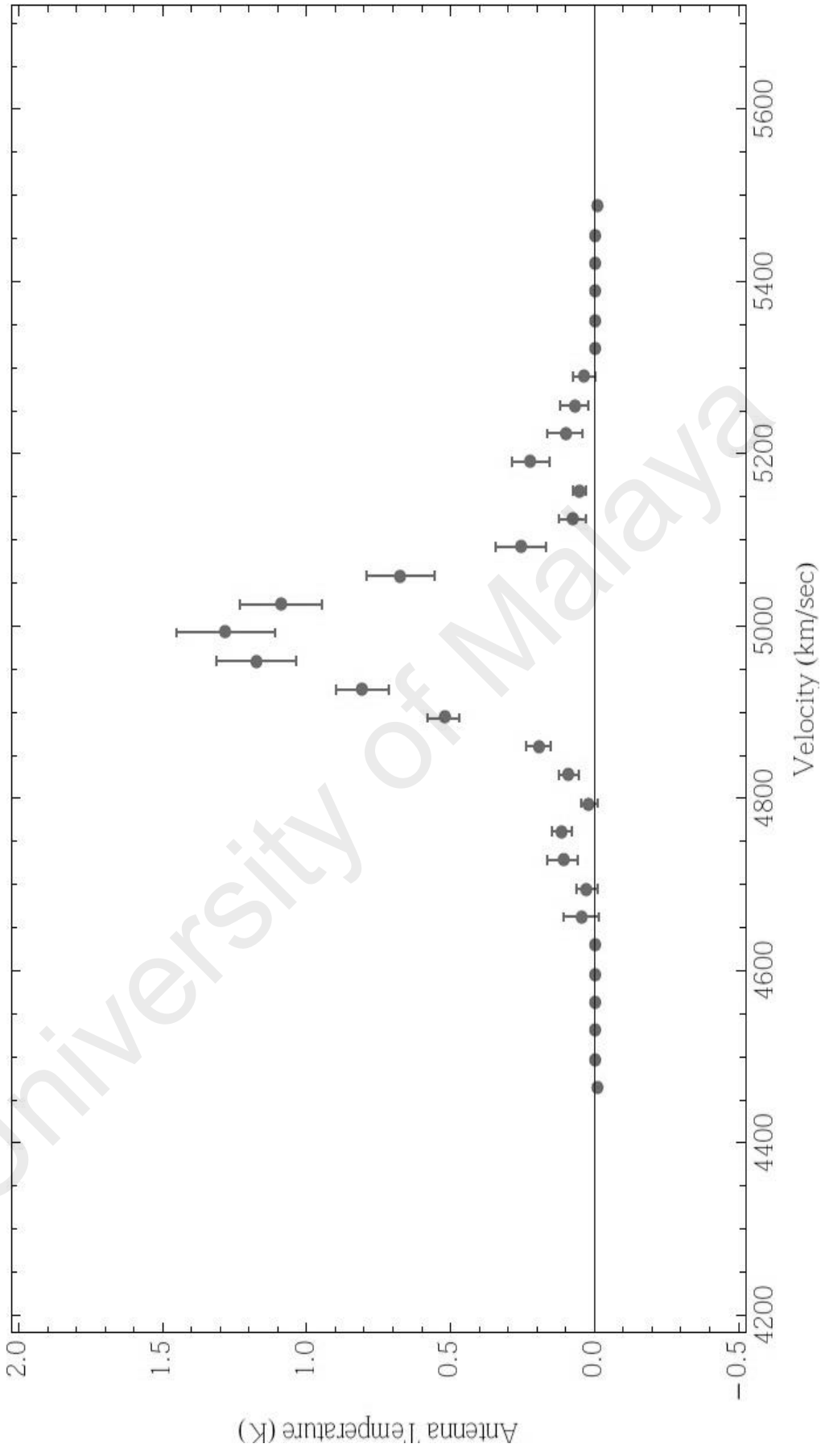

Figure 4.6 The binning of final integrated spectrum of A262 with error bars

4.2.6 M_{HI} in A262

The M_{HI} has been calculated by using the information acquired from the observation. The peak temperature obtained from the observation is (1.1403 ± 0.0089) K. Then, the temperature was later being converted into radio flux density. After the conversion, the flux density of A262 calculated to be about 0.654 Jy. By applying equation (4) in Section 1.3, the M_{HI} value of A262 has been calculated to be about $(6.22 \pm 0.32) \times 10^{11}$ $M_{\odot}$.

4.3 Archival Data

4.3.1 Cluster Membership

The total stellar mass, ΣM_i and virialized mass, M_{VT}, have been deduced according to velocity range obtained from HI observation in this study. The velocity range of A262 that is being considered in this study is 4450 km/s < v < 5300 km/s, based on Figure 4.6. Thus, the estimation of ΣM_i and M_{VT} are only restricted in this velocity range. However, before one can calculate ΣM_i and $M_{VT,}$ it is worth to find out the total number of galaxies falls in the velocity range in a given radius (R = 69 arcmin). Hence, the determination of cluster membership is significant.

The galaxies fell in 4450 km/s < v < 5300 km/s is listed in Table 4.2. There are 62 objects listed in NASA/IPAC Extragalactic Database (NED) within radius, R = 69 arcmin. However, seven objects have been omitted because they are a pair of galaxies, which were not taken into account in stellar mass and virialized mass calculations. Hence, only 55 individual galaxies are being considered into the calculation of ΣM_i and M_{VT}. As mentioned, to obtain accurate mass estimation require one to remove any interlopers present in the data. The direct method has been chose in this study for interloper's removal. The first step should be taken is by plotting a histogram of number of galaxies falls into certain range of redshifts (or velocity).

Table 4.2 The list of galaxies in A262 within radius, R = 69 arcmin and velocity range 4450 km/s < v < 5300 km/s. RA and Dec are measured according to epoch 2000.

Object Name	RA (°)	Dec (°)	Redshift, $z \pm \Delta z$	Separation (arcmin)
NGC 708	28.19	36.15	0.016195 ± 0.000053	0.871
NGC 705	28.17	36.14	0.015057 ± 0.000040	1.807
NGC 704 NED01	28.17	36.12	0.015778 ± 0.000020	2.598
NGC 704 NED02	28.17	36.13	0.015771 ±0.000020	2.822
NFP J015228.0+360926	28.12	36.16	0.015691 ±0.000120	3.806
2MASX J01524952+3614515	28.21	36.25	0.016501 ± 0.000037	6.097
2MASX J01523447+3600462	28.14	36.01	0.016205 ± 0.000060	8.629
NGC 700	28.07	36.04	0.015264 ± 0.000030	9.443
CGCG 522-045	28.35	36.01	0.016118 ± 0.000030	10.489
2MASX J01524785+3619365	28.20	36.33	0.016688 ± 0.000057	10.527
2MASX J01534075+3605459	28.42	36.10	0.016945 ± 0.000040	10.590
CGCG 522-044	28.31	36.33	0.016588 ± 0.000027	12.291
MCG +06-05-021	27.94	36.13	0.015000 ± 0.000040	12.434
2MASX J01530937+3620455	28.29	36.35	0.016698 ± 0.000027	12.585
2MASX J01535138+3612130	28.46	36.20	0.014977 ± 0.000040	12.774
NGC 717	28.48	36.23	0.016571 ± 0.000267	13.972
VI Zw 95	28.42	36.13	0.015708 ± 0.000033	14.708
NFP J015258.7+362545	28.24	36.43	0.016521 ± 0.000073	16.838
NFP J015150.7+355243	27.96	35.88	0.015484 ± 0.000080	19.907
2MASX J01522797+3629533	28.12	36.50	0.015177 ±0.000030	21.602
UGC 1350	28.24	36.51	0.016745 ± 0.000030	22.501
2MASX J01515325+3629077	27.97	36.49	0.014907 ± 0.000043	23.397
V Zw 126	27.89	35.88	0.016455 ± 0.000027	22.632
UGC 1308	27.71	36.28	0.017249 ± 0.000027	25.273
2MASX J01541177+3630434	28.55	36.51	0.016084 ± 0.000060	27.395
IC 1732	27.07	35.93	0.016235 ± 0.000040	27.886
CGCG 522-049	28.64	36.56	0.015607 ± 0.000031	27.908
UGC 1387	28.80	36.26	0.015144 ± 0.000011	29.137
2MASX J01545507+3552279	28.73	35.87	0.016298 ± 0.000157	30.015
NGC 687	27.64	36.37	0.016982 ± 0.000027	30.770
2MASX J01502423+3620256	27.60	36.34	0.016451 ± 0.000183	31.701
V Zw 116	27.56	36.23	0.017262 ± 0.000103	31.769

KUG 0149+353	28.00	35.64	0.016541 ± …..	32.061
UGC 1366	28.58	36.63	0.017055 ± 0.000027	34.141
2MASX J01505167+3540341	27.72	35.68	0.016068 ± 0.000123	37.063
KUG 0150+365	28.46	36.79	0.015631 ± 0.000045	40.304
UGC 1392	28.87	36.56	0.017606 ± 0.000264	40.586
KUG 0151+352	28.05	35.53	0.016692 ± …..	40.757
NGC 679	27.43	35.79	0.016842 ± 0.000030	43.525
V Zw 131	28.03	35.41	0.016268 ± 0.000267	44.764
UGC 1353	28.35	36.96	0.017525 ± 0.000077	48.978
UGC 1415	29.18	36.38	0.015600 ± 0.000200	49.180
CGCG 522-061	28.74	36.87	0.016788 ± 0.000062	50.462
MRK 1010	28.74	35.42	0.015401 ± 0.000284	50.601
CGCG 522-083	29.24	35.95	0.015974 ± 0.000054	51.439
2MASX J01534805+3659000	28.45	36.98	0.017309 ± 0.000187	51.543
KUG 0153+353	29.17	35.59	0.017445 ± 0.000023	57.137
UGC 1434	29.41	36.26	0.015144 ± 0.000103	58.564
UGC 1257	27.03	36.45	0.015544 ± 0.000009	59.996
NGC 753	29.43	35.92	0.016355 ± 0.000007	60.578
NGC 759	29.46	36.34	0.015567 ± 0.000047	61.608
GALEXASC J014733.81+360427.7	28.14	36.07	0.015794 ± 0.000009	63.402
CGCG 522-068	28.91	37.04	0.015961 ± 0.000200	63.413
UGC 1251	26.88	36.04	0.016168 ± 0.000027	65.047
KUG 0155+361	29.57	36.35	0.015880 ± …..	66.707

Clear pictures regarding the existence of interlopers in the cluster have been represented by plotting the distribution of the individual galaxies as a function of right ascension (RA) and declination (Dec) as shown in Figure 4.7. Based on the plotting, the galaxies are concentrated in a region near the cluster center and become less dense in the region far from the center. Although the plotting gives the information of how the galaxies distributed throughout the field, several steps in determining the presence of interlopers and directly remove them for better estimation mass of the cluster also being provided in this study.

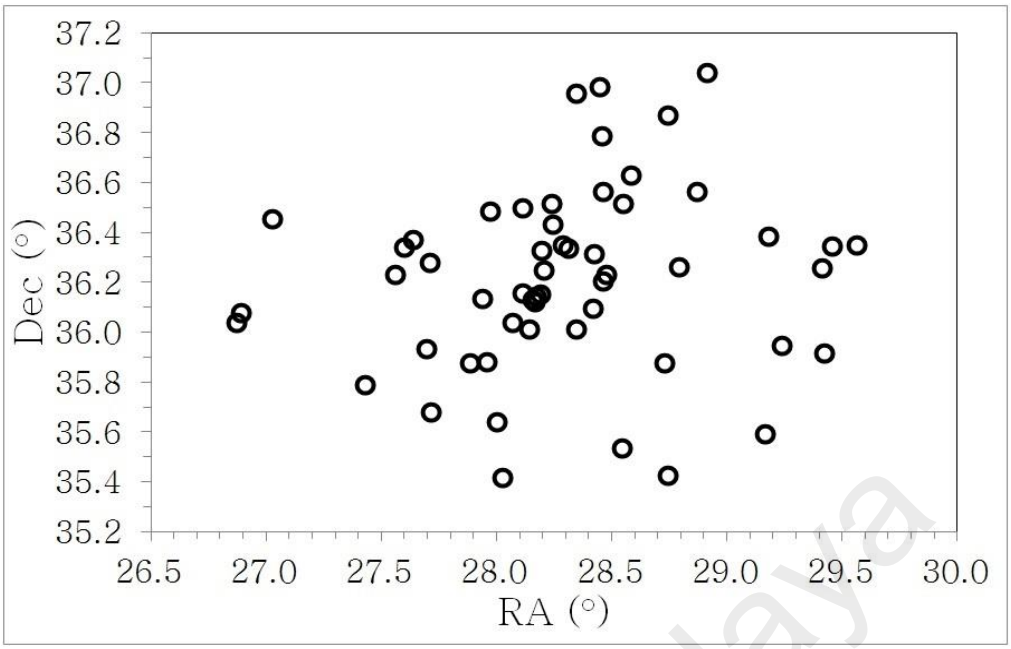

Figure 4.7 The distribution in the sky of galaxies with measured redshifts in the region of A262 (R = 69′) as a function of RA and Dec

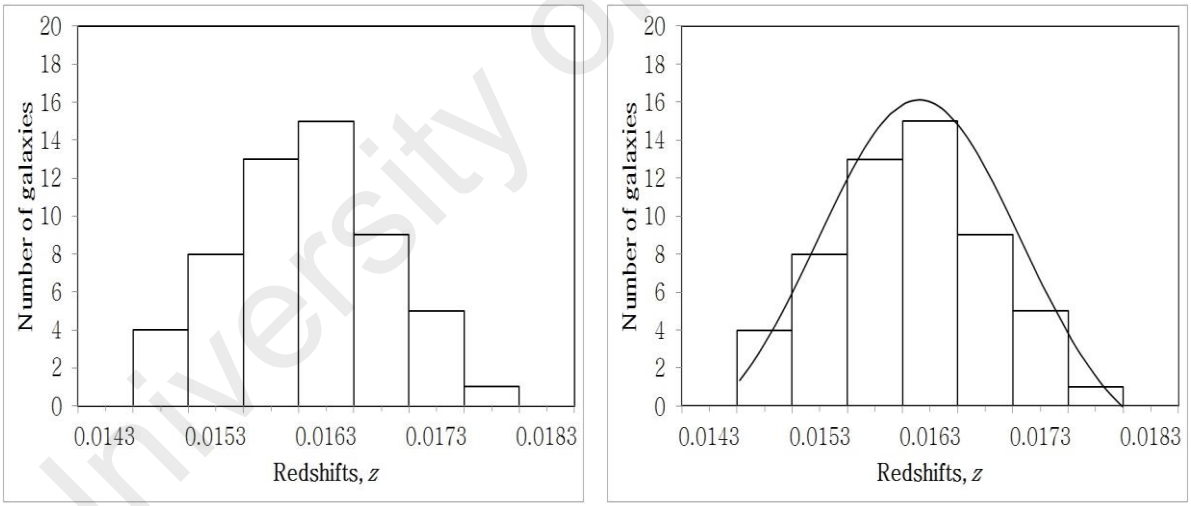

Figure 4.8 Redshifts distribution in A262. Left: Measured redshift distribution of A262 within range of 0.0143 – 0.0183. Right: Measured redshift distribution of A262 within the range 0.0143 – 0.0183 together with overlapped-Gaussian fitting, centered at the mean redshift, z = 0.01635

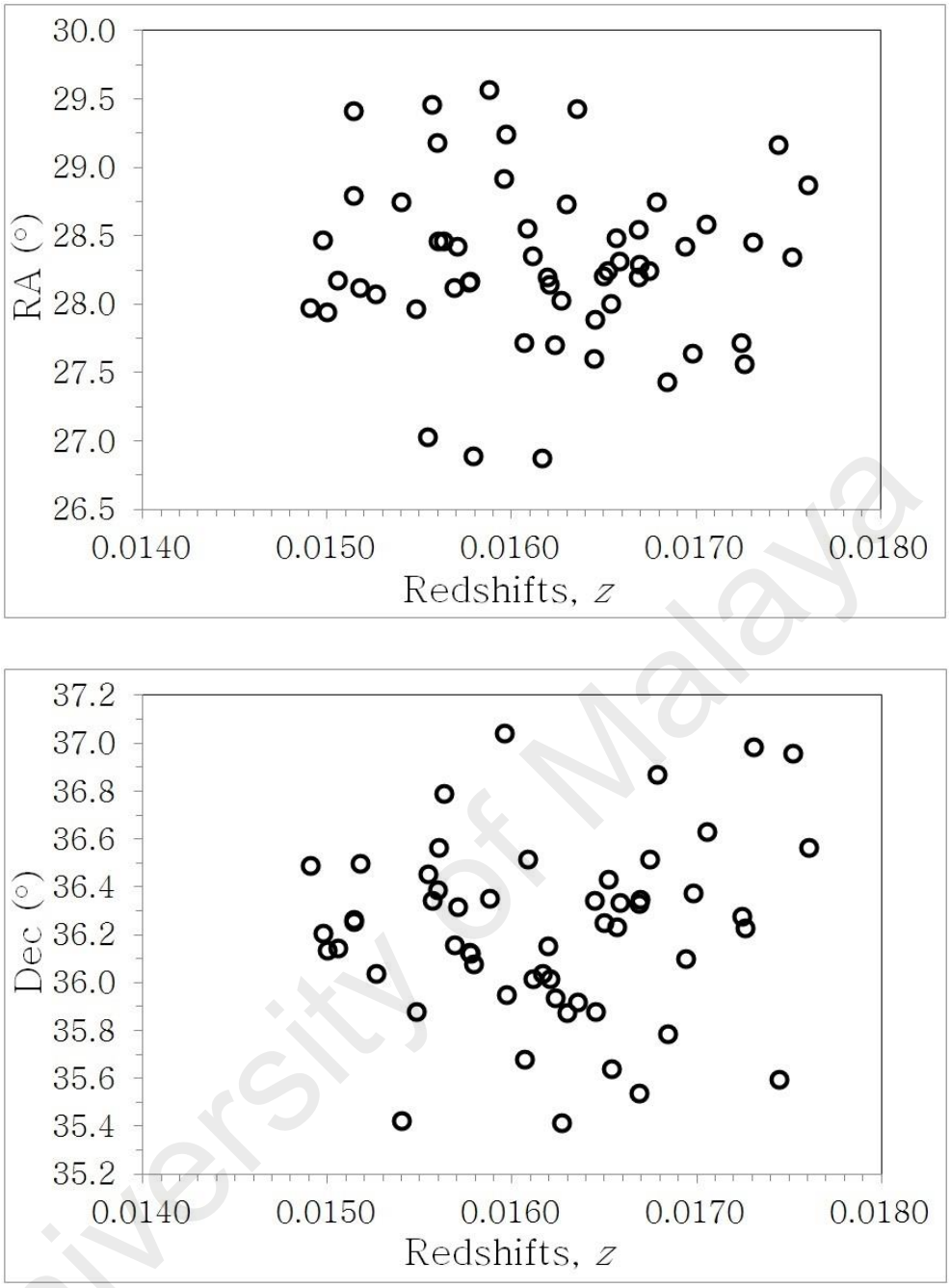

Figure 4.9 Redshifts distribution for the combined dataset of 55 galaxies as a function of RA (top) and Dec (bottom) respectively, measured in degrees

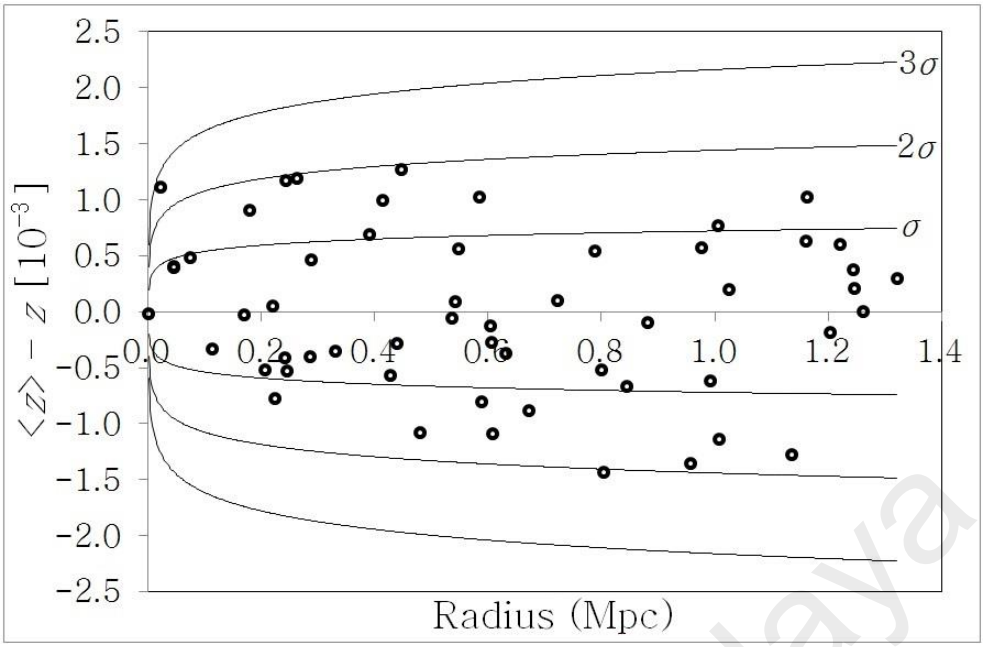

Fig. 4.10 Velocity diagram of A262 with standard deviation limit of σ, 2σ and 3σ

From the figures above, one can conclude that there is no interloper or outlier exists in the dataset of given radius and velocity range. Thus, all the galaxies in a given boundary is said to be a part of cluster A262 without any foreground or background in a line-of-sight to the cluster. However, only 47 galaxies were accounted for ΣM_i and M_{VT} since some of the information required for the estimation is not available.

4.3.2 Total Stellar Mass, ΣM_i, Virialized Mass, M_{VT} and Dark Matter Mass, M_{DM}, in A262

The number of galaxies should be included into total stellar mass calculation and virialized mass calculation is 47 – neglecting 8 galaxies with no data available for the calculations. Table 4.3 lists the galaxies that had been considered in the calculation of two parameters mentioned above. However, in the calculation, the radius of the cluster should be converted into Mpc (or metre). Hence, the unit conversion for the radius of the cluster is given by 100 kpc = 4.910 arcmin. It has been calculated that 69 arcmin is equivalent to 1.4 Mpc (or 4.34×10^{22} metres).

Table 4.3 The list of galaxies of 47 galaxies in A262

Object Name	Velocity, $V \pm \Delta V$ km/s	K_s (2MASS), $K_s \pm \Delta K_s$ mag.	Flux density, $S_\nu \pm \Delta S_\nu$ Jy ($\times 10^{-3}$)	Stellar mass, M_i ($\times 10^{10} M_\odot$)
NGC 708	4855 ± 16	8.57 ± 0.03	248.00 ± 6.01	26.56
NGC 705*	4514 ± 12	14.50 ± 0.40	6.75 ± 3.01	0.10
NGC 704 NED01	4730 ± 6	13.88 ± 0.24	1.87 ± 0.46	0.19
NGC 704 NED02	4728 ± 6	10.38 ± 0.03	47.20 ± 1.37	4.73
2MASX J01524952+3614515	4947 ± 11	13.89 ± 0.18	1.86 ± 0.34	0.21
2MASX J01523447+3600462	4858 ± 18	14.22 ± 0.21	1.37 ± 0.30	0.15
NGC 700	4576 ± 9	11.21 ± 0.04	21.90 ± 0.86	2.05
CGCG 522-045	4832 ± 9	11.25 ± 0.05	21.10 ± 0.96	2.22
2MASX J01534075+3605459	5080 ± 12	13.62 ± 0.16	2.38 ± 0.37	0.28
CGCG 522-044	4973 ± 8	11.43 ± 0.04	17.90 ± 0.69	2.00
2MASX J01530937+3620455	5006 ± 8	12.41 ± 0.07	7.22 ± 0.50	0.82
2MASX J01535138+3612130	4490 ± 12	14.04 ± 0.21	1.62 ± 0.35	0.15
NGC 717	4968 ± 80	10.43 ± 0.03	44.80 ± 1.21	5.02
2MASX J01522797+3629533	4550 ± 9	13.00 ± 0.10	4.21 ± 0.42	0.39
UGC 1350	5020 ± 9	10.20 ± 0.05	55.60 ± 2.62	6.33
2MASX J01515325+3629077	4469 ± 13	12.53 ± 0.10	6.48 ± 0.63	0.58
V Zw 126	4933 ± 8	12.25 ± 0.07	8.40 ± 0.56	0.92
UGC 1308	5171 ± 8	9.25 ± 0.03	134.00 ± 3.37	16.08
2MASX J01541177+3630434	4822 ± 18	12.78 ± 0.11	5.16 ± 0.56	0.40
IC 1732	4867 ± 12	10.27 ± 0.04	52.10 ± 1.81	5.54
CGCG 522-049	4679 ± 9	12.39 ± 0.09	7.39 ± 0.65	0.72
UGC 1387	4540 ± 3	12.76 ± 0.12	5.25 ± 0.61	0.49
2MASX J01545507+3552279	4886 ± 47	11.51 ± 0.05	16.50 ± 0.76	1.79
NGC 687	5091 ± 8	9.24 ± 0.02	135.00 ± 2.50	15.71
2MASX J01502423+3620256	4932 ± 55	12.57 ± 0.08	6.23 ± 0.46	0.68
V Zw 116	5175 ± 31	11.92 ± 0.07	11.40 ± 0.72	1.38
KUG 0149+353	4959 ± …	12.39 ± 0.11	7.39 ± 0.80	0.82
UGC 1366	5113 ± 8	10.30 ± 0.04	50.80 ± 1.66	6.00
2MASX J01505167+3540341	4817 ± 37	13.44 ± 0.16	2.80 ± 0.45	0.29
KUG 0150+365	4686 ± 13	11.45 ± 0.07	17.50 ± 1.11	1.71
UGC 1392	5278 ± 79	11.25 ± 0.06	21.20 ± 1.29	2.69
NGC 679	5049 ± 9	9.14 ± 0.02	148.00 ± 3.30	16.88
V Zw 131	4877 ± 80	10.89 ± 0.04	29.30 ± 1.13	3.12

UGC 1353	5254 ± 23	10.22 ± 0.02	54.60 ± 1.22	6.85
UGC 1415	4677 ± 60	10.29 ± 0.03	50.90 ± 1.52	5.03
CGCG 522-061	5033 ± 19	11.13 ± 0.04	23.70 ± 0.89	2.71
MRK 1010	4617 ± 85	12.88 ± 0.17	4.68 ± 0.80	0.45
CGCG 522-083	4789 ± 16	11.24 ± 0.05	21.30 ± 1.09	2.20
2MASX J01534805+3659000	5189 ± 56	12.08 ± 0.08	9.78 ± 0.76	1.17
KUG 0153+353	5230 ± 7	12.16 ± 0.10	9.12 ± 0.89	1.14
UGC 1434	4540 ± 31	10.88 ± 0.04	29.80 ± 1.06	2.75
UGC 1257	4660 ± 3	11.30 ± 0.05	20.10 ± 1.03	1.95
NGC 753	4903 ± 2	9.37 ± 0.02	119.00 ± 2.54	12.97
NGC 759	4667 ± 14	9.14 ± 0.02	147.00 ± 2.60	14.46
CGCG 522-068	4785 ± 60	11.64 ± 0.07	14.70 ± 0.91	1.52
UGC 1251	4847 ± 8	10.97 ± 0.05	27.40 ± 1.21	2.87
KUG 0155+361	4761 ± …	12.63 ± 0.11	5.92 ± 0.61	0.61

The total stellar mass, ΣM_i, for 47 galaxies in A262 is calculated to be about (1.84 ± 0.07) × 10^{12} $M_\odot$. The total stellar mass shows the lower limit for A262 should provide, since the calculation neglected the 8 members of the cluster – because lack of information. Meanwhile, the velocity dispersion, σ, for 47 galaxies in A262 is calculated to be about (215.73 ± 23.59) km/s. By inserting the value of σ into equation (1), the virialized mass of A262 within radius, R = 69 arcmin (or 1.4 Mpc), has been deduced to be about (7.16 ± 0.09) × 10^{13} $M_\odot$. By using equation (3), the dark matter mass also has been deduced to be about (6.19 ± 0.08) × 10^{13} $M_\odot$, which equivalent to ~ 97% of dark matter content in the cluster.

4.3.3 Galaxy Morphology

The distribution of different morphological types of galaxies has been plotted since the plot gives a good estimate to the location of HI in cluster of galaxies. Figure 4.11 shows the distribution of different morphological types of galaxies in A262 within R = 69 arcmin. The morphological types in the figure is divided into elliptical (E), irregular (Irr), spirals (S and SB), lenticulars (S0) an unidentified morphology, denoted as N/A.

The distribution of different morphological types of galaxies shows a good tracer in determining the location of neutral hydrogen gas in boundary given.

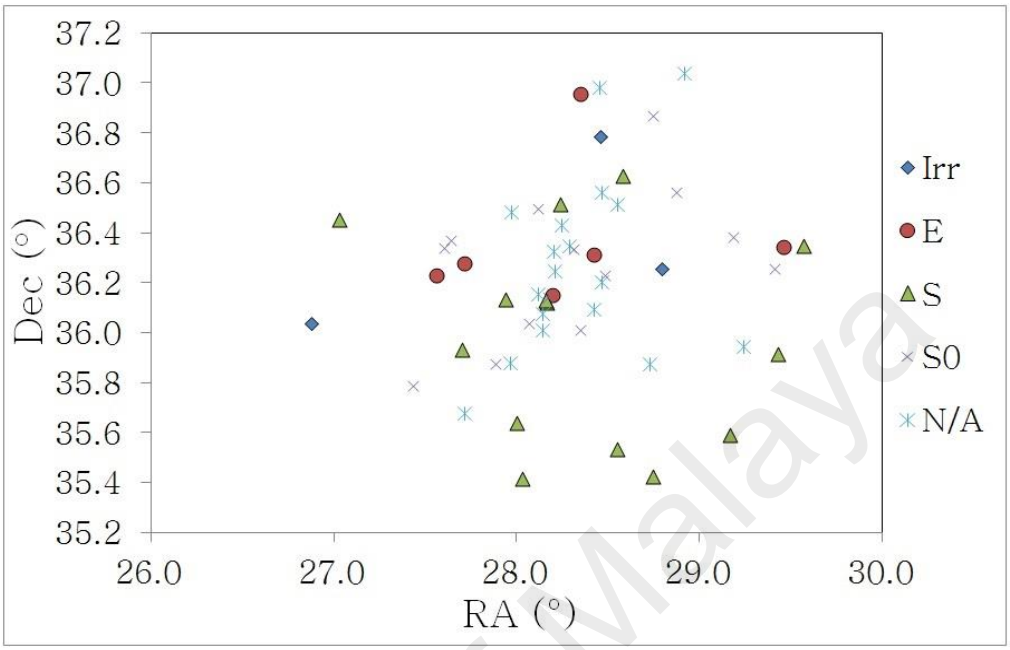

Figure 4.11 The distribution of different morphological types of galaxies for 55 galaxies in A262 within R = 69 arcmin

CHAPTER 5 DISCUSSION AND CONCLUSION

5.1 Redshift Distribution

Beside in determining the cluster membership in a cluster, redshift distribution analysis provides a verification on HI data obtained using 7-metre radio telescope. According to Haynes et al. 1997, HI spectral line observation also can be used to precisely determine the value of redshift. By comparing data acquired from both HI spectral line observation and archival observation, the final integrated spectrum in Figure 4.6 shows peak velocity at (4970 ± 0.53) km/s, which is equivalent to redshift of [0.0166 ± (1.767×10^{-6})] . Compare to the reference value of redshift of A262 stated in Chapter 3, this is slightly 2% more than the expected value. In fact, the redshift from Struble & Rood, 1999, that was determined in optical band, this newly defined redshift of A262 was obtained based on HI spectral line observation. This is fairly good agreement with the relation stated by Haynes et al., 1997. Thus, this provides higher level of confidence to the fact that the data obtained from the observation is strictly from A262, despite of minuscule error.

A262 has two mean redshifts based on optical data, where $\langle z_{21} \rangle$ = [0.0166 ± (1.767×10^{-6})] (from observation) and $\langle z_{opt} \rangle$ = [0.0162 ± (7.4×10^{-5})], respectively, and small line-of-sight velocity dispersion σ = (215.73 ± 23.59) km/s. σ presented in this study is somehow smaller compared to previous studies since the radius extends more than a few parsec. The calculation of σ for cluster A262 is restricted to a given boundary obtained in the study. The low value of σ_{los} also represents that A262 resembles the characteristics of young cluster, as suggested by Jones & Forman, 1991. It translates that A262 undergone merger between its neighbours. The neighobours around A262 vicinity might fall towards the gravitational potential well of A262 to form much larger structure.

5.2 Contribution of M_{HI} in A262

The contribution of neutral hydrogen mass by using methodology described in Chapter 3 should depend on other parameters mentioned in Chapter 1, which are total stellar mass, virialized mass and finally dark matter mass. In Chapter 4, these masses have been deduced to be about $(1.84 \pm 0.07) \times 10^{12}\ M_{\odot}$, $(7.16 \pm 0.09) \times 10^{13}\ M_{\odot}$ and $M_{DM} = (6.91 \pm 0.08) \times 10^{13}\ M_{\odot}$, respectively. In addition, the mass of neutral hydrogen has been calculated to be $(6.22 \pm 0.32) \times 10^{11}\ M_{\odot}$. One can grasp the contribution of HI gas in A262 by taking a ratio between these parameters. The percentage of M_{HI} to the total mass of the cluster, i.e. M_{VT} (or M_{HI}/M_{VT}) is about ~ 1%. This firmly shows that majority of matter in the cluster is not in the form of baryonic HI mass and is less than the findings from previous works that 3 – 5% baryonic HI component contributes to the total mass of the cluster. The value of the percentage is slightly different from the accepted value because the study only covers a certain area of the cluster. Since the missing dark matter mass is believed to dominate the total mass of the cluster, the percentage of M_{HI} to M_{DM} is slightly lower than ~ 1%. Moreover, the percentage of M_{HI} to the total stellar mass, i.e. ΣM_i (or $M_{HI}/\Sigma M_i$) is about ~ 34%. This provides a strong insight that only about 20 – 40% of total baryonic matter in a cluster is in the form of HI gas, while the rest exists in the other forms.

The telescope being used in this study covered 65% of the total area of the cluster. The discrepancies exist in some of the values in the previous paragraph shows that the capability of the telescope was quite limited to cover up the whole area of the cluster. For example, the M_{HI} of A262 should vary between $(5.7 – 7.2) \times 10^{12}\ M_{\odot}$, hence provides 8 – 10% of HI to the total mass of the cluster. This gives off approximately 75% of HI mass that resides outside the beamwidth of the telescope. In addition, the accumulated mass of A262 should reach up to ~ $10^{14}\ M_{\odot}$. Due to limited number of galaxies accounted in this study – according to spectroscopic analysis – covered by the

beamwidth of the telescope, the accumulated mass of A262 is one magnitude lower than expected i.e. 10^{13} $M_{\odot}$. One should expect the accumulated mass of A262 could reach up 10^{14} $M_{\odot}$ if the beam size of the telescope is increased.

The minuscule percentage of M_{HI} obtained in this study compared to the other three masses might be due to some reasons stated below:

(a) Again, the capability of the telescope plays a significant role in determining the total neutral hydrogen mass in the cluster. Since the telescope is restricted to a certain boundary of a given radius, the M_{HI} estimated in this study mainly focus in the area of the cluster surrounded by the beam size of the telescope. The total area of the cluster retrieved from NED is about 211 arcmin. However, the θ_{FWHM} obtained from the observation on a certain object in the sky yields to 138 arcmin. This is in fact gives rise to the conclusion that the telescope was only able to observe the centre of the cluster. The velocity of A262 acquired in this study is about 4970 km/s, slightly higher than the center of the cluster, NGC708 with v = 4898 km/s, by 72 km/s.

(b) Since the heart of the cluster consists of highly energetic particles that can be observed through X-ray, most of the HI gas – especially in spirals – is being stripped away catastrophically from the cluster center. This hot emitting X-ray gas evolves the neutral hydrogen gas into ionized HII gas. This confirms in the less amount of neutral HI gas at the area restricted in this study, since the study mainly focused at the center of the cluster with high percentage of hot gas. If the size of the hot gas is comparable to the total size of the cluster, a large reservoir of ionized HII gas will be created and the amount of neutral HI gas will drop substantially.

(c) From the diagram on morphological types of galaxies in A262 (Figure 4.11), it is renowned that most of spirals – which rich in HI gas – tend to locate themselves at the outskirt of the cluster. Other types of galaxies, such as ellipticals and lenticulars, which have less contribution on HI gas, will be found at the center of the cluster.

The usage of small radio telescope equipped with HI spectral line receiver is somehow important in determining the lower limit of HI contribution in cluster of galaxies. With the advancement of instrument's construction and data handling, the HI line observation by using small radio telescope can be lifted up to higher degree of accuracy. Therefore, the study has shown that the methodology being implemented is relevant into empowering the technique of radio astronomy in astrophysical research.

REFERENCES

Baan, W. A., Haschick, A. D., and Burke, B. F. (1978). *The Astrophysical Journal, 225*: 339-342

Bahcall, N. A. (1977). *Annual Review of Astronomy & Astrophysics, 15*: 505

Bahcall, N. A. (1988). *Proceedings of the 130th Symposium of the International Astronomical Union*

Bahcall, N. A. (1996). *in Astrophysical Quantities*, ed. A. Cox (New York: *AIP*)

Bahcall, N. A. (1998). *Physica Scripta, 85*: 32-36

Battye, R. A., Davies, R. D., and Weller, J. (2008). *Monthly Notices of the Royal Astronomical Society, 355*: 1339-1347

Bertram, T., Eckart, T., Krips, M., Staguhn, J. G., and Hackenberg, W. (2006). *Astronomy & Astrophysics, 446*: 29-42

Bell, E. F., and de Jong, R. S. (2001). *The Astrophysical Journal, 550*: 212-229

Beiging, J. H. and Biermann, P. (1977). *Astronomy & Astrophysics, 60*: 361-368

Binney, J., and Tremaine, S. (2007). *Princeton University Press*. ISBN: 978-0-691-13027-9

Bîrzan, L., Rafferty, D. A., McNamara, B. R., Wise, M. W., and Nulsen, P. E. J. (2004). *The Astrophysical Journal, 607*: 800-809

Biviano, A., Metcalfe, L., McBreen, B., Kneib J. -P., Altieri, B., Delaney, M., Elbaz, D., Kessler, M., Leech, K., Okumura, K., Ott, S., and Schulz, B. (2003). *Memorie della Società Astronomica Italiana, 74*: 266

Bravo-Alfaro, H., Szomoru, A., Cayatte, V., Balkowski, C., and Sancisi, R. (1997). *Astronomy & Astrophysics Supplement Series, 126*: 537-546

Bregman, J. N., McNamara, B. R., and O'Connell, R. W. (1990). *The Astrophysical Journal, 326*: 639-644

Briggs, F. H. (2003). *World Scientific*: 1-17

Butcher, H., and Oemler, A. (1978). *The Astrophysical Journal, 219*: 18

Caldwell, R. R. Dave, R., and Steinhardt, P. J. (1998). *Physical Review Letters, 80*: 1582-1585

Carroll, T. A. (2007). *Proceedings of Solar Modern Facilities - Advanced Solar Science, 297*

Cox, T. J. and Loeb, A. (2008). *Monthly Notices of the Royal Astronomical Society, 386*: 461-474

Dahlem, M. (2005). *Astronomy & Astrophysics, 429*: L5-L8

Davies, R. D., and Lewis, B. M. (1973). *Monthly Notices of the Royal Astronomical Society, 165*: 231-244

Dresslar, A. (1980). *The Astrophysical Journal, 236*: 351

Dressler, A. (1984). *Annual Review of Astronomy & Astrophysics, 22*: 185-222

Einstein, A. (1915). *Zeitschrift für Mathematik und Physik, 63*: 215-225

Einstein, A. (1936). *Science, 84*: 506–507

Faber, S. M., and Gallagher, J. S. (1979). *Annual Review of Astronomy & Astrophysics, 17*: 135-187

Field, G. B. (1959). *The Astrophysical Journal, 129*: 525

Frieman, J. A., Turner, M. S., and Huterer, D. (2008). *Annual Review of Astronomy and Astrophysics, 46*: 385-432

Giovanelli, R., Haynes, M. P., and Chincarini, G. L. (1982). *The Astrophysical Journal, 262*: 442-450

Girardi, L., Bressan, A., Bertelli, G., and Chiosi, C. (2000). *Astronomy & Astrophysics Supplement Series, 141*: 371-383

Gunn, J.E., and Gott, J. R. (1972). *The Astrophysical Journal, 176*: 1

Hartle, J. B., and Hawking, S. W. (1983). *Physical Review D, 28*: 2960-2975

Haynes, R. F., Jauncey, D. L., Murdin, P. G., et al. (1978). *Monthly Notices of Royal Astronomical Society, 185*: 661

Haynes, M. P., Giovanelli, R., Herter, T., Vogt, N. P., Freudling, W., Maia, M. A. G., Salzer, J. J., and Wegner, G. (1997). *The Astronomical Journal, 113*: 1197-1211

Hubble, E. P. (1929). *Proceedings of the National Academy of Science United States of America, 15*: 168

Johnston-Hollitt, M., Hunstead, R. W., and Corbett, E. (2008). *Astronomy & Astrophysics, 479*: 1-8

Ibrahim, U. F. S. U., Abidin, Z. A., and Hassan, M. S. R. (2017). *New Astronomy (in prep.)*

Jones, C., and Forman, W. (1991). *Advance Space Research, 10*: 209

Kaiser, N. (1998). *The Astrophysical Journal, 498*: 26-42

Kalberla, P. M. W., Mebold, U., and Reif, K. (1982). *Astronomy and Astrophysics, 106*: 190

Kalloglyan, A. T. (1971). *Astrofizika, 8*: 43-51

Koehler, J. A., and Robinson, B. J. (1966). *The Astrophysical Journal, 146*: 488-503

Koribalski, B., Whiteoak, J. B., and Houghton, S. (1995). *Proceedings of the Astronomical Society of Australia, 12*: 20-25

Kroupa, P., Famaey, B., de Boer K. S., Dabringhausen, J., Pawlowski, M., Boily C. M., Jerjen, H., Forbes, D., Hensler, G., Metz, M. (2010). *Astronomy & Astrophysics, 523*: 32

Lin, Y-T., Mohr, J. J., and Stanford, S. A. (2003). *The Astrophysical Journal, 591*: 749

Matthew, F. (2013). *Arstechnica*

Merritt, D. (1987). *The Astrophysical Journal, 313*: 121-135

Moss, C., and Dickens, R. J. (1977). *Monthly Notices of the Royal Astronomical Society, 178*: 701-715

Oort, J. H. (1932). *Bulletin of the Astronomical Institute of the Netherlands, 6*: 249

Oort, J. H. (1960). *Bulletin of the Astronomical Institute of the Netherlands, 15*: 45

Oort, J. H. (1983). *Annual review of Astronomy & Astrophysics, 21*: 373-428

Peebles, P. J. E. (1993). *Princeton University Press*. ISBN: 978-0-691-01933-8

Penzias, A. A. ,and Wilson, R. W. (1965). *The Astrophysical Journal, 142*: 419-421

Perea, J., del Olmo, A., and Moles, M. (1990). *Astronomy & Astrophysics, 237*: 319-328

Perlmutter, S., Schmidt, B. P., and Riess, A. G. (2011). *Nature, 7*: 833

Peterson, B. M., Craine, E. R., and Strittmatter, P. A. (1978). *Publications of the Astronomical Society of the Pacific, 90*: 386-392

Pratap, P., and McIntosh, G. (2005). *American Journal of Physics, 73*: 399-404

Planck Collaboration et al. (2014). *Astronomy & Astrophysics, 571*: A1

Planck Collaboration et al. (2016). *Astronomy & Astrophysics, 594*: A13

Roberts, M. S., and Haynes, M. P. (1994). *Annual Review of Astronomy & Astrophysics, 32*: 115-152

Roberts, W. W. Jr. (1975). *Vistas in Astronomy, 19*: 91-109

Rood, H. J. (1988). *Annual Review of Astronomy & Astrophysics, 26*: 245-294

Rubin, V. C., Ford, W., and W. Kent, Jr. (1970). *The Astrophysical Journal, 159*: 379

Sakai, S., Giovanelli, R., and Wegner, G. (1994). *The Astronomical Journal, 108*: 33-43

Sarazin, C. L. (1998). *X-ray Emission from Clusters of Galaxies, Cambridge Astrophysics Series*

Schechter, P. (1976). *The Astrophysical Journal, 203*: 297-306

Schröder, A., Drinkwater, M. J., and Richter, O. -G. (2001). *Astronomy & Astrophysics, 376*: 98-111

Shostak, G S., van der Kruit, P. C., Hummel, E., Shaver, P. A., and van der Hulst, J. M. (1982). *Astronomy & Astrophysics, 115*: 293-307

Slipher, V. M. (1913). *Lowell Observatory Bulletin, 2*: 56

Slipher, V. M. (1917). *Proceedings of the American Philosophical Society, 56*: 403-409

Smith, S. (1936). *The Astrophysical Journal, 83*: 23-30

Stroe, A., Oosterloo, T., Röttgering, H., Sobral, D., van Weeren, R., and Dawson, W. A. (2015). *Monthly Notices of Royal Astronomical Society, 452*: 2731-2744

Struble, M. F., and Rood, H. J. (1999). *The Astrophysical Journal Supplement Series, 125*: 35-71

Voit, G. M. (2005). *Reviews of Modern Physics, 77*: 207-258

Williams, D. R. W. (1973). *Astronomy & Astrophysics Supplement Series, 8*: 505-516

Wojtak, R., Łokas, E. L., Mamon, G. A., Gottlöber, S., Prada, F., and Moles, M. (2008). *Astronomy & Astrophysics*, *466*: 437-449

Yahil, A., and Vidal, N. V. (1977). *The Astrophysical Journal, 214*: 347-350

Zwicky, F. (1933). *Helvetica Physica Acta, 6*: 110-127

Zwicky, F. (1937). *Publications of the Astronomical Society of the Pacific, 49*: 204

Zwicky, F. (1958). *l'Astronomie, 72*: 285

LIST OF PUBLICATIONS AND PAPERS PRESENTED

M. S. R. Hassan, Z. Z. Abidin, U. F. S. U. Ibrahim, N. Hashim & D. A. A. Lee, "Redshifts Distribution in A262", *Monthly Notices of Royal Astronomical Society (MNRAS)* (ISI Journal), Feb 2016

N. Hashim, Z. Z. Abidin, U. F. S. U. Ibrahim, Z. S. Hamidi, R. Umar, **M. S. R. Hassan**, "The Nonlinear Least Square Fitting for Rotation Curve of Orion Dwarf Spiral", *Sains Malaysiana* (ISI Journal), Aug 2014

M. S. R. Hassan, Z. Z. Abidin, Z. A. Ibrahim, U. F. S. U. Ibrahim & N. Hashim, "Measuring the Neutral Hydrogen Mass of Galaxy Cluster A262", *American Institute of Physics (AIP)* (Conference Proceeding), National Physics Conference (PERFIK), Nov 2013

M. S. R. Hassan, Z. Z. Abidin, U. F. S. U. Ibrahim, N. Hashim & Z. A. Ibrahim, "Possible Candidates for Dark Matter in Galaxy Cluster", Non-Scorpus AKEPT (Conference Proceeding), AYRC Conference, Dec 2011

U. F. S. U. Ibrahim, Z. Z. Abidin, N. Hashim, **M. S. R. Hassan** & Z. A. Ibrahim, "Determining the Dark Matter Content of Dwarfs and Dwarfs Spheroidal Galaxies in the Local Group Cluster using the CAS Parameters", IEEE (Conference Proceeding), Aug 2011